Lunds Universitets Naturgeografiska Institution

Seminarieuppsatser Nr. 67

Estimation of the Soil Moisture Distribution in the Tamne River Basin, Upper East Region, Ghana

Per Asserup
&
Martin Eklöf

2000

Department of Physical Geography,
Lund University
Sölvegatan 13, S-221 00 Lund,
Sweden

Abstract

Northern Ghana experiences one dry season per year, but severe droughts may occur more infrequently. This is of concern to the local farmers of the Tamne River Basin (northeast Ghana) who depend on adequate rainfall amounts during the rainy season. Unfavourable precipitation amounts may lead to catastrophic consequences. It is therefore crucial to develop methods for predicting the distribution of soil moisture in the region. In this way, locations more sensitive to drought may be delineated.

A high quality DEM was constructed over the region as topography is considered to be an important control on soil moisture. This was accomplished by combining elevation and linear features representing streams in the interpolation routine. The importance of topography relative to soil moisture was examined by using an index that reflects both the specific drainage area and local slope. As soil type and vegetation are also characteristics controlling the hydrologic response of a catchment, they were also included as two simple indices. The aforementioned variables were evaluated against 94 soil samples, distributed along seven transects, from which soil moisture was derived.

The analysis showed that a statistical model that provides consistent results in terms of predicting soil moisture distribution was difficult to achieve for the entire basin. Only one statistical model was applicable to the whole basin; the one including soil texture. It is of limited utility however, since detailed data concerning the spatial distribution of soil properties was not available. The assumptions underlying the construction and use of the wetness index limit its application to homogeneous sub-basins. This is shown by the more reliable results from the transects. Topography is shown to be less influential than expected. Conversely, soil texture provided the key for mapping the distribution of soil moisture under wet conditions.

Keywords: *GIS, hydrological modelling, topography, wetness index, soil moisture*

ACKNOWLEDGEMENTS

This study was made possible through the financial support from SIDA and its Minor Field Study (MFS) program administrated by SLU Uppsala, and through the cooperation between the Department of Physical Geography at Lund University, and the Department of Geography & Resource Development at University of Ghana, Legon, for all of which we are most grateful.

In Ghana:
We would like to thank Prof Paul Yankson at the Department of Geography & Resource Development for his kind cooperation and assistance prior to and during our stay in Ghana.

Dr Paul Bomber Tanzubil at SARI Manga (Savanna Agricultural and Research Institute), for providing lodging, equipment and means of transportation as well as contacts with the local authorities.

Opoku Pabi for his kind assistance during the fieldwork, but also for guidance throughout our stay. Sebastian Agorkle, for his assistance in the soil laboratory and for being great company at the SARI Guest House. Daniel, the caretaker at the SARI Guest House, for cooking excellent meals and for carrying heavy loads of water whenever necessary. Iddisah Amadu, the SARI driver, for his excellent driving skills and impressive soil drilling contributions.

Last, but not least, we would like to acknowledge the Ph D students at the computer laboratory in the Department of Geography & Resource Development, for us feeling welcome and for contributing with ideas and suggestions in our work.

In Sweden:
We would like to thank our supervisor, Karin Larsson, for taking care of practical arrangements before our departure to Ghana, and for being available for questions and guidance. We would also like to acknowledge Dr Lars Eklundh and Dr Petter Pilesjö for providing valuable suggestions and comments. Dr Petter Pilesjö for providing the Topoform software.

We would also like to thank SLU Uppsala and Monica Halling for the services they have provided.

TABLE OF CONTENTS

1 INTRODUCTION

During the recent decades, Ghana has experienced several years of missgrowth related to drought. Between the years 1982 and 1984, severe conditions caused the total yearly cereal production to decrease from 518 000 to 450 000 tons (Allotey et al., 1998). Upon this, years followed when the domestic food production increased. In 1990, however, the drought returned, which resulted in a massive loss of production for most crops (Internet 1).

Due to the unimodal precipitation characteristics of northern Ghana, farmers in these territories are totally dependent on the amount of precipitation available during the short period of the rainy season, between April and September. A deviation from the yearly average precipitation sometimes causes a reduction, or even total collapse of the cereal production. In general, the variability of rainfall is higher the more arid a region is. This means that the fluctuations in precipitation are expected to be greater in northern Ghana than in the southerly parts (Dickson & Benneh, 1995).

Due to the physical characteristics of a landscape, different parts of the terrain receive different quantities of soil moisture. Since plants are reduced to using only the soil water storage during droughts, it is desirable to estimate the spatial distribution in soil moisture. The resulting soil moisture maps can be used as a tool in environmental decision-making (Western et al., 1999).

The hydrological response of a catchment to rainfall is largely influenced by topography (Barling et al., 1994). Considering the accessibility of topographic data in general, and the ease of which topographic attributes can be derived from these, it is valuable to find a suitable method for estimations of the spatial distribution in soil moisture, using topography as primary input. The most common implementation within this context is the topographic wetness index, often referred to as the TOPMODEL-index since it is used in TOPMODEL to represent topographic heterogeneity (Beven & Kirkby, 1979).

The topographic wetness index describes the spatial variation in depth to the groundwater table. Since the soil moisture content in the root zone is governed by depth to the water table to a large degree (Grip & Rodhe, 1994), the index can be used to assess the spatial soil water status in an area (Rodhe & Siebert, 1999). According to Blöschl & Sivapalan (1995), the predictive ability of the topographic wetness index has not been entirely investigated. In studies where the topographic wetness index has been evaluated against measured soil moisture contents, the correspondence has been relatively low (Western et al., 1999).

Modern GIS software packages often provide tools for calculations of topographic wetness indices, but often in an oversimplified way. The implementations often lack realistic descriptions of flow directions in an area, which constitutes the foundation in computation of indices. The one-directional flow algorithms included in most programs cannot model the dispersion of water properly. It is therefore desirable to go further and explore the advantages of multi-directional flow algorithms that account for the distribution of water in eight possible directions (Burrough & McDonnell, 1998).

1.1 Aim

The main objective of this study is to assess the possibilities of estimating the spatial distribution in soil moisture in a semi-arid environment of low relief, using topography as primary input data. Intermediate goals in the study are:

- Construction of a reliable Digital Elevation Model
- Determination of the predictive ability of topographic attributes for estimation of the soil moisture distribution, focused on the topographic wetness index, computed in standard GIS-software and in more theoretically realistic non-standard applications
- Assessment of the relative importance of topography in distributing the soil moisture compared to soil texture and vegetation
- Development of a statistical model for prediction of the soil moisture distribution in the Tamne River Basin of the Upper East Region, Ghana

Limitations include the simplification in representation of the soil and vegetation, but also time constraints in terms of results not being applicable all year round. Soil samples were collected over a period of two weeks in October of 1999, which means that they are season specific.

1.2 The Physical Geography of Ghana

1.2.1 Geography & Climate of Ghana

Ghana can be divided into five physiographic regions, each of which are showing similar patterns of relief: the coastal plain, the forest dissected plateau, the savanna high plains, the Voltaian sandstone basin and the ridges and escarpments bordering the former (Dickson & Benneh, 1995). The major parts of the Ghanaian territory are low-lying, with a few peaks near the Togo border (Instituto del Tercer Mundo, 1999).

Tropical forest used to cover 34 per cent of the country's surface, but it is now only a quarter of its original size and 42 per cent of today's "forests" are in fact timber plantations, immature trees and weed. Plantations of cocoa, coffee, banana and oil palm trees are common in these areas (Instituto del Tercer Mundo, 1999).

Fresh water resources are estimated at 53.2 km^3 per year, consisting of 30.3 km^3 of internally produced water and 22.9 km^3 per year of run-off from other countries. The drainage network of Ghana is divided into the Volta river system, the southwestern river basins and the coastal rivers (Internet 3). The Volta, Ghana's main river, has an artificial lake formed by the Akosombo dam (Instituto del Tercer Mundo, 1999).

Ghana is fairly well off with water resources, but there is a high variability in the amount of available water within the year and over several years (Internet 2). The pattern of rainfall is closely related to the movement of the ITCZ (Dickson & Benneh, 1995). Figure 1 shows the yearly rainfall totals and the yearly mean temperatures for Ghana.

The southern parts of the country experience two rain seasons resulting in more than 2000 mm of precipitation annually. These bimodal peaks occur between April and July, and between September and November (Holmertz, 1996). The mT (Tropical Maritime Air) air mass originates from the southern Atlantic Ocean, where it gathers the moisture that is later to be released in heavy showers, mainly in the southern regions of Ghana. This regime is also generally associated with clouds that prevent part of the solar radiation from reaching the land surface and keeps the surface temperature stable throughout the day. The average day temperature in the south is usually around 25ºC during the mT regime. The moist air mass reaches the northern regions only once a year, when it is heavily charged with water vapor and when the sun is at the Tropic of Cancer (Dickson & Benneh, 1995). The single rain period occurs between April and September and brings around 1100 mm of precipitation (Holmertz, 1996).

The northeasterly wind of Harmattan (cT, Tropical Continental Air) is initiated when the sun is positioned around the Tropic of Capricorn, i.e. when the ITCZ has moved to the south of the equator (Dickson & Benneh, 1995). The cT causes a long period of drought in the north, stretching from October through March (Holmertz, 1996). The Harmattan originates from the Sahara-Arabian desert, where the transport over dry areas explains its dryness. Day temperatures in the north may, during this period, exceed 40ºC, while it drops considerably during the night (Dickson & Benneh, 1995).

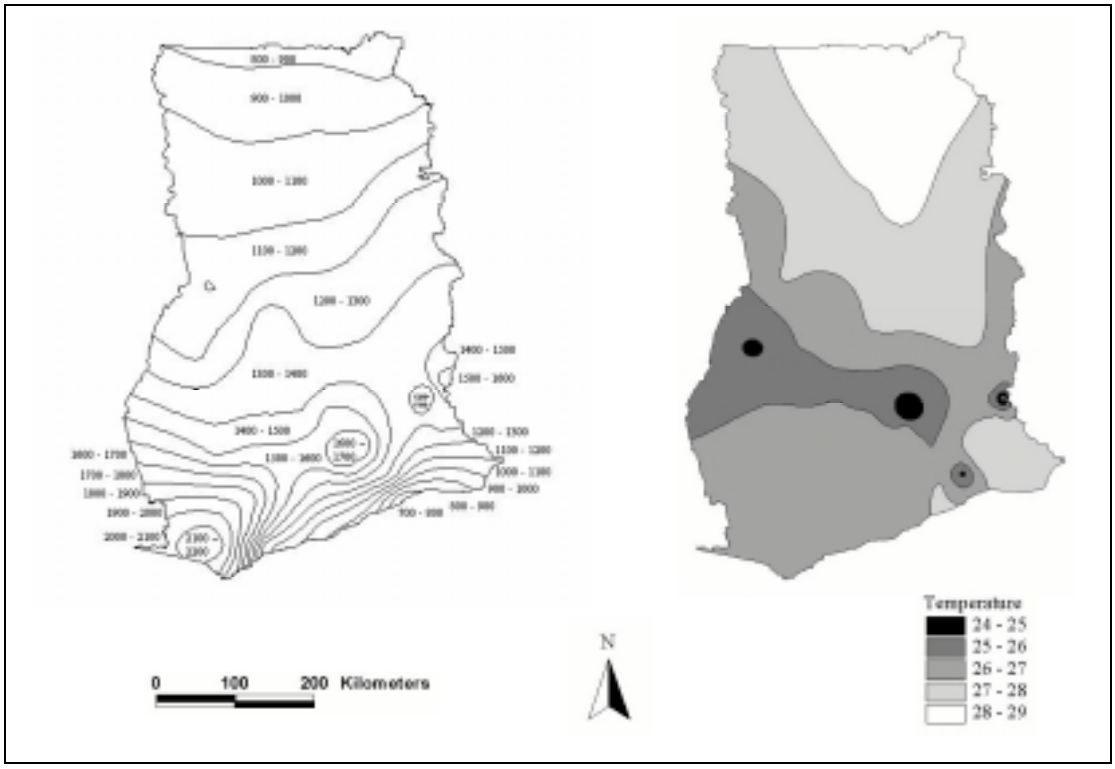

Figure 1. *Yearly rainfall totals (mm) and yearly mean temperatures (°C) for Ghana (CAG, 1999).*

1.2.2 Geology

The Ghanaian geology consists of rock from eras stretching from 4500 million years ago until recent times. Among the common ones, the Dahomeyan formation originates from the Precambrian, and is now the foundation in the southeast coastal plains consisting of gneisses and schists. The most important geological formation in Ghana is the Birrimian, made up by phyllites, schists and metamorphosed lavas underlying more than 75% of the forest zone. It contains all of the minerals exported from the country, among which gold, diamonds, manganese and bauxite are the most important (Instituto del Tercer Mundo, 1999). Extensive masses of granite occur in belts where it probably appeared in a melted state parallel to the Birrimian. Also originating from the Precambrian are the Tarkwaian, the Togo and the Buem formations, found in narrow basins stretching from the north to the south and consisting of mainly sedimentary rocks. The Palaeozoic era produced the Voltaian formation, consisting of flat-bedded or horizontal sedimentary rock that covers approximately 40% of the Ghanaian land surface (Dickson & Benneh, 1995).

1.2.3 Soils & Agriculture

Soil erosion was first surveyed in the 1930's, and during the last 30 years, it has become an important form of land degradation. Some 70% of the land surface is subject to severe or moderate sheet or gully erosion and about 40% of this occurs in the northern savanna (Internet 3).

The base upon which the Ghanaian soils have been developed are weathered parent materials where nutrients have been leached out for a long time. Declining soil fertility is now also threatening the agricultural production, and further, the population

pressure has reduced the former 8-15 year fallow period to 2-3 years on a 1-3 year cropping basis (Internet 3).

The major soils include, according to the FAO system (Allotey et al., 1998):

- *Plinthic Acrisol* (ferric), oxisols found in rain forest areas with an excess rainfall of 1800 mm
- *Rodic Ferralsol*, ochrosols in forest and savanna environments with a precipitation of between 900 and 1650 mm
- *Plinthic Ferralsol*, groundwater laterites consisting of a layer of sandy to silty loam upon an iron pan in "upland locations"
- *Pellic Vertisols*, tropical black earths made up by dark clay in savanna areas with rainfall ranging from 1000 to 1300 mm
- *Gleyic Solenetz*, tropical grey earths consisting of grey hard soils, are found in savanna environments over acid rocks with precipitation of between 600 and 900 mm

In 1996 more than 1/3 of the Ghanaian cultivable land was utilized compared with 1/5 in 1987 (Internet 3), and the agriculture is based on self-contained, privately owned pieces of land. The main export is cocoa, and since the 1980's the World Bank has contributed with monetary resources to make the production efficient. Still, difficulties include inertia in the cultivators and an inefficient marketing. Other commercial exports include tobacco, cotton and rubber, but they are also affected by the country's economic difficulties as well as the ever-changing weather. The situation is similar for base crops like: maize, rice, millet, sorghum, yams, cassava and plantain (Holmertz, 1996).

Ghana's meat production is found in the stock raising of the north, but it is deficient for the needs of the country. The fish supplies in the sea and in Lake Volta are good, but they feed only half of the population. It is the lack of cold storage and transport that prevents the development of the fishery industry. The government aims at food self-sufficiency no later than in the year 2000 (Holmertz, 1996).

1.3 Study Area

1.3.1 Location

The Tamne River Basin (approximately 800 km^2) is located in the Upper East Region of Northern Ghana, close to the Togo border in the east and Burkina Faso in the north (lat. 10°50'N - 11°05'N, long. 0°00'W - 0°30'W) (figure 2). Bawku, situated on the water divide in the northern part of the Tamne River Basin, is the administrative capital of the area and the trading market for the local farmers as well as foreign cattle merchants. The SARI/Manga Agricultural Station is located a few kilometers to the southwest from Bawku in a relatively densely cultivated part of the catchment. Garu Natinga, sited approximately 20 kilometers to the southeast of Manga on the other side of Tamne River, is one of the major villages in the basin.

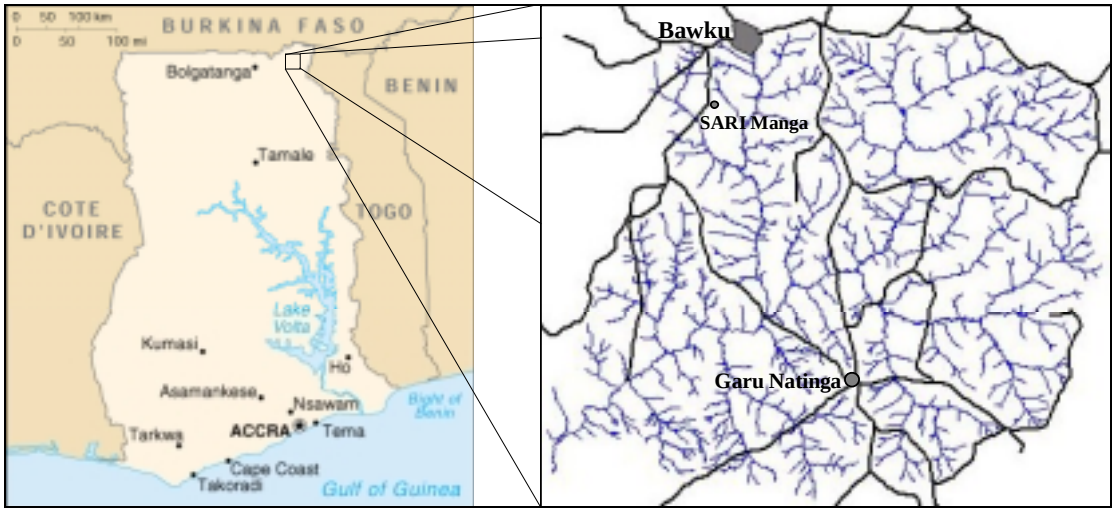

Figure 2*. The Tamne River Basin is situated in the very north east of Ghana. The administrative capital of the area is Bawku, whereas Garu Natinga is one of the major villages in the catchment. The SARI Manga agricultural station is located a few km to the south of Bawku.*

1.3.2 Topography & Drainage

Figure 3 shows the topography and the drainage network of the Tamne River Basin. The altitude of the catchment ranges from 150 to 360 meters, with a gently sloping terrain towards the southwest, but the landscape rises slightly as the Gambaga Escarpment is approached to the south. No specific topographic features can be noted, except from a Birrimian hill formation, with the highest elevations in the basin.

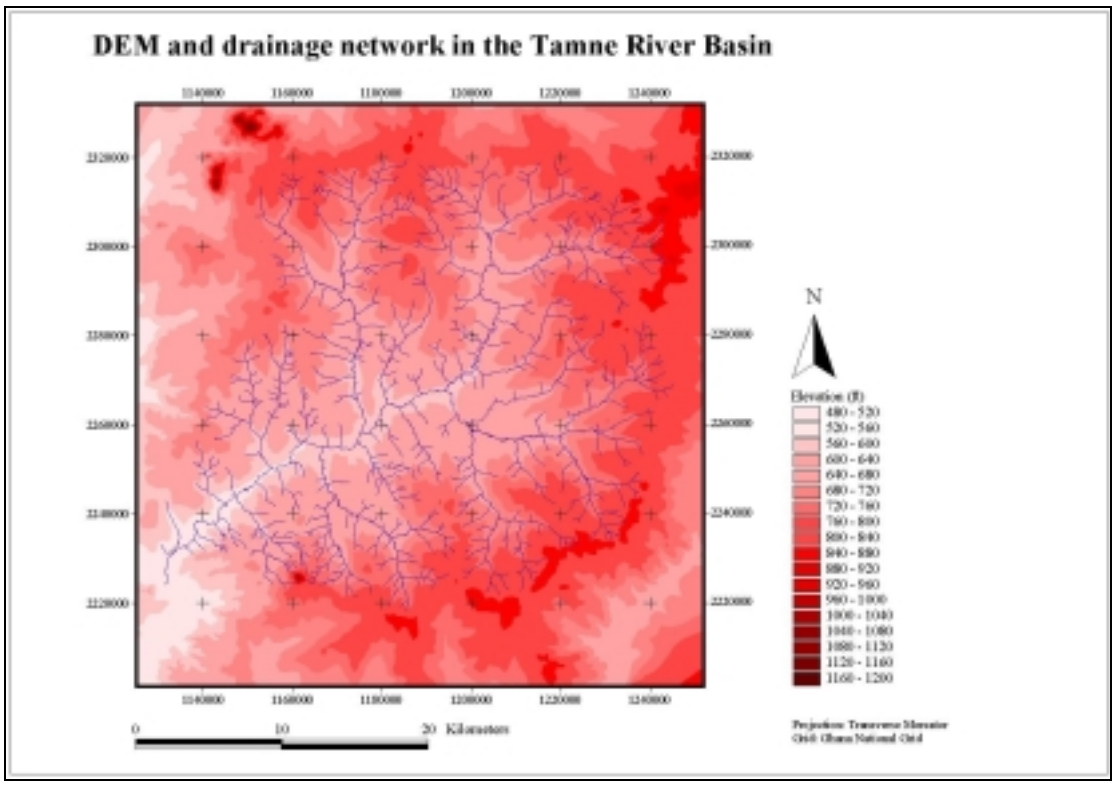

Figure 3. *The topography and drainage of the Tamne River Basin (elevation in feet).*

The landscape is otherwise clearly shaped by the Tamne River, whose previous and present flow paths constitute the lowest points in the terrain. The Tamne River, which is a tributary of the White Volta, varies greatly in its extent and flow intensity throughout the year and between years. Not all of the existing flow channels carry water all year round; some are filled only during the rain season or on occasions of extreme precipitation. A few of the flow paths are also subject to dam constructions for later use of the water in irrigation during the dry season.

1.3.3 Geology

Most of the soils present in the upper part of the slopes are formed by in situ weathering of coarse and fine grained biotite granite and hornblende granite, and in many places the soil is underlain by decomposed granite. These originate from intrusive complexes formed during the Precambrian. The Birrimian rocks, occurring mainly in the hill complex in the southwest, were folded and intruded in a northeast-southwesterly direction under the earlier stages of the Precambrian. This process was followed by heavy erosion and the Birrimian complex was subsequently overlaid by Voltaian sandstones and shale of younger age. A mix of granites and Birrimian rocks underlies an area stretching from Manga and continuing to the north, which occasionally can be seen as rock outcrops (FAO, 1967). The riverbed foundation consists of mixed quartzites and sandstones presumably originating from deposition.

1.3.4 Agricultural Practices

Due to an increased population pressure, the farming system has transformed from a system of shifting cultivation to a permanent farming system, referred to as compound farming. This system is centered on a couple of huts, i.e. the compound, around which the cultivation of crops and vegetables takes place. Water availability is a crucial factor when it comes to crop production in the area, and a loss of 20 – 30% of the production is normal. Water stress is the main reason for this, but also insufficient storage facilities (Madsen & Hulmose Nielsen, 1991). Irrigation from the previously mentioned dam reservoirs occurs as joint ventures between farmers, while drinking water is gathered manually from a large number of drilled and sealed boreholes, as well as from a few open wells.

The most common crops in the area are millet (*Pennisetum americanum*) and sorghum (*Sorghum bicolor*), both of which are cultivated for their grains and for the hay (figure 4). Millet matures quickly with no more than 300 mm of precipitation, and cutting or grazing can begin 4-6 weeks after sowing. The crop can reach 3 meters in height and may be cultivated on sandy soils where it utilizes nutrients and water deep below the surface. The growing conditions for sorghum are similar to those of millet, but it reaches a stem height of around 2 m. It is grown for forage as well as for grain in drier areas, and the grains can also be used for starch extraction (Internet 4).

Instead of the conventional crops, maize has been introduced by the agricultural authorities as a more output efficient alternative, and is now commonly appearing throughout the landscape. Its protein content is higher than that of sorghum and millet, but it also demands more water why it is cultivated with a higher risk of crop failure (Cunin, 1993). Other crops include: groundnuts, bambara beans, cowpeas, yams and rice.

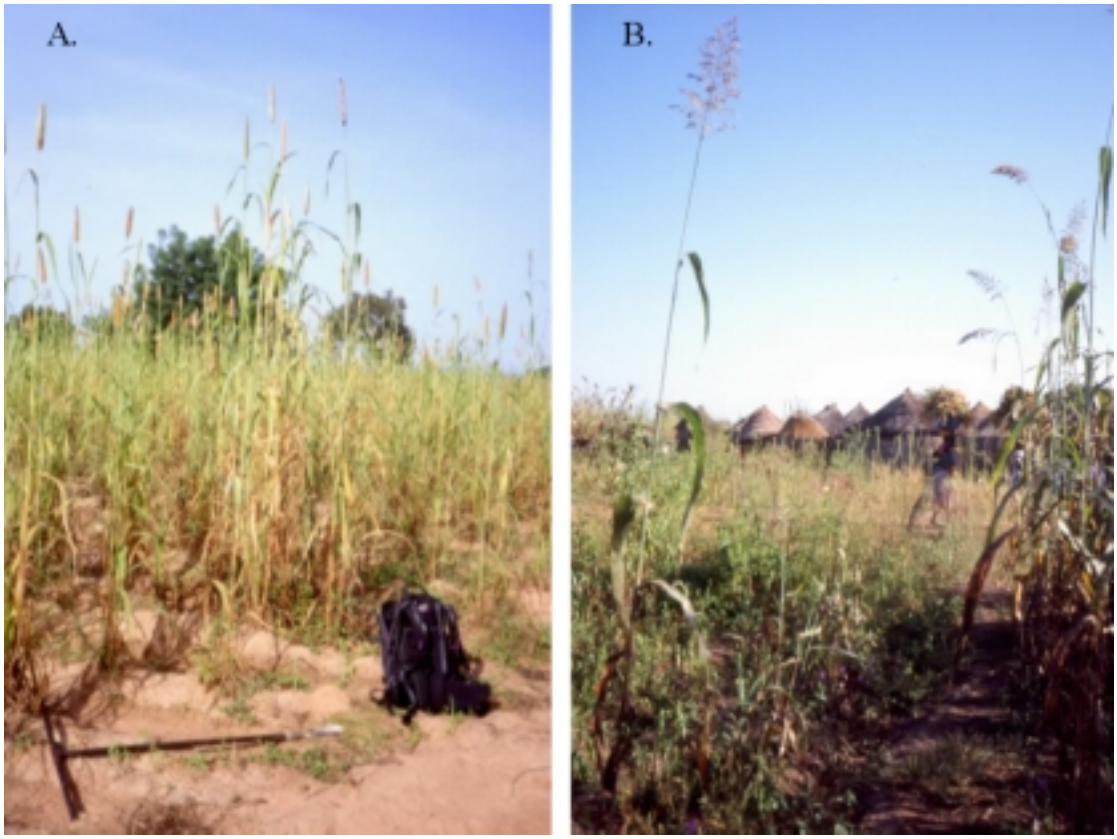

Figure 4. *Millet (A), one of the most commonly occurring crops in the Tamne River Basin and Sorghum (B), another base crop, in the vicinity of a family compound.*

1.3.5 Soils

The types of soils found within the Tamne River Basin are of three main categories: moderately well drained upland soils, concretionary or non-concretionary, shallow iron pan soils and poorly and imperfectly drained mixed alluvial and colluvial soils (FAO, 1967) (Appendix 1).

The non-concretionary soils of the uplands average 0.45 to 0.75 meters in depth and are found on the upper and middle part of the slopes. The soil is underlain by a soft concretionary pan or iron concretions mixed with clay loam or sandy clay to form a matrix. During the rainy season this soil type is almost saturated, as opposed to the dry season when the soil becomes exceptionally dry, apart from the underlying soft pan that retains some moisture. The texture of the topsoil ranges from loamy sand to sandy loam, while the subsoil is dominantly sandy clay loam. Due to the low (5 – 10 percent) clay content of the topsoil, infiltration rates are fairly high compared with the subsoil, where a higher content of clay put a stop to high percolation losses. The soil is considered as moderately suitable for agriculture (FAO, 1967).

The concretionary soils of the uplands, reaching a depth of 0.9 meters, are found on eroded and undulating terrain. The topsoil consists of concretionary sandy loam with a high content of iron concretions (50 percent iron concretions and 50 percent soil matrix in the uppermost part of the soil). In the downward direction, the clay content and the amount of concretions increase (FAO, 1967).

The shallow iron pan soils are found in the upper part of the terrain and average 0.15 to 0.3 meters in depth. Below this depth, a hard vesicular pan is present. The soil is light textured with small concretions and considered not suitable for farming (FAO, 1967).

The imperfectly drained mixed alluvial soils are found on lower slopes. They have a light textured topsoil (from coarse sand to sandy loam) and a medium textured subsoil (sandy clay loam to sandy clay). The infiltration rate of the topsoil is high but decreases from 0.6 meters and below. The poorly drained alluvial soils are found on valley bottoms. Their texture varies from silty clay to clay with some calcium and carbonate concretions in the subsoil. Below 1.8 meters, a sandy layer at varying depth underlies the soil. Due to the high content of clay, the infiltration rate is particularly slow. The heavy textured part of the alluvial soils is suitable for cultivation of rice, while areas with a more light textured soil can be used for cultivation of other crop types. The main drawback of these soils is their prolonged wet status during part of the year, which has to be compensated by drainage and some leveling/terracing in order to offer suitable conditions (FAO, 1967).

1.3.6 Climate

The Tamne River Basin has an average temperature of approximately 27°C. The hottest months are February through May when the temperature often exceeds 30°C. Figure 5 shows mean monthly rainfall totals and mean monthly temperature for the period 1961 – 1990. The area is clearly characterized by a single maximum regime, with peak precipitation from July to September. The inter-annual variability in total precipitation is significant. Figure 6 shows monthly rainfall totals for the year of 1983 (a dry year) and 1989 (a wet year). The difference in total amount of precipitation between these years is 437 mm. The values presented here were recorded at the SARI/Manga meteorological station, located in the northern part of the Tamne River Basin.

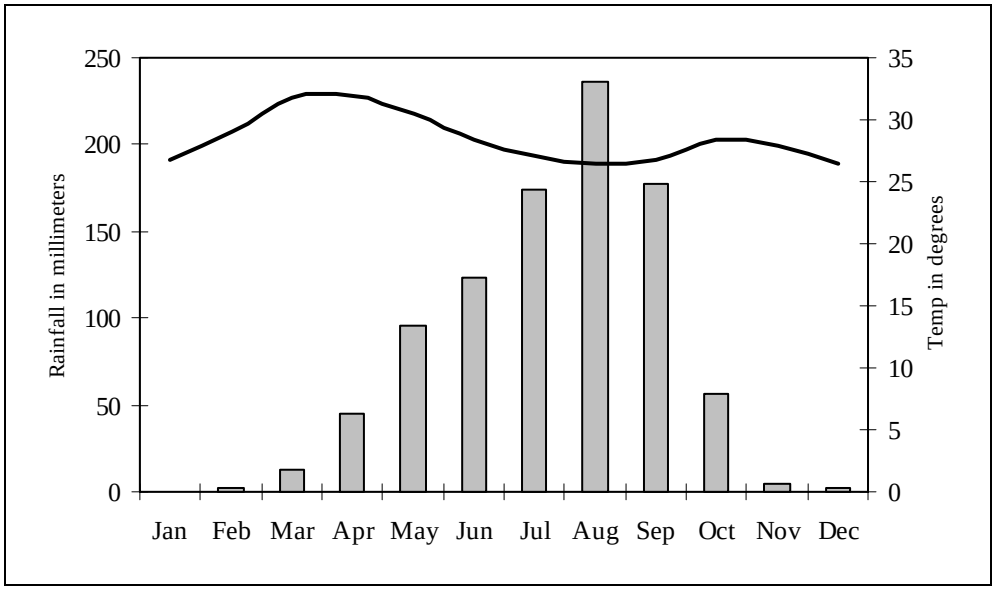

Figure 5. *Mean monthly rainfall totals and mean monthly temperature for the years 1961 – 1990, recorded at SARI Manga meteorological station.*

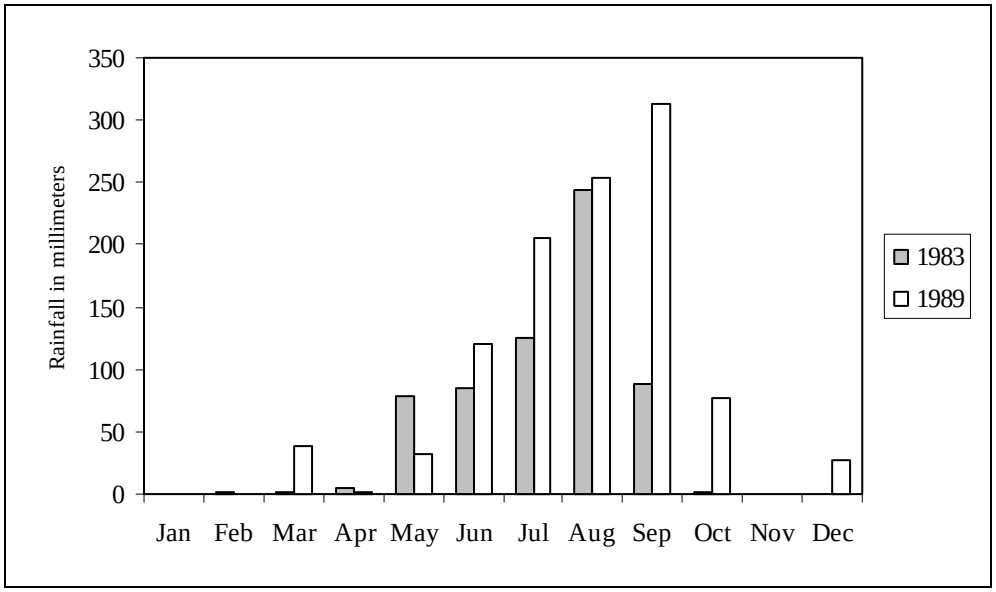

Figure 6. *Monthly rainfall totals for the years 1983 and 1989, recorded at the SARI Manga meteorological station.*

1.3.7 Vegetation

Appendix 2 illustrates the different vegetation classes found within the Tamne River Basin as described in the Country at a Glance database. The most widespread vegetation types are open cultivated savanna woodland and widely open cultivated savanna woodland. The differences between these classes are their location and tree density. Areas of open cultivated savanna woodland are mostly present at low elevations within the catchment, in connection to the main drainage channels and circumscribed by widely open cultivated savanna woodland at higher levels. The approximate tree density of the first class is 11 to 20 trees/ha, whereas the latter has around 6 to 10 trees/ha. Other less extensive vegetation classes found within the area are: open forest with less than 60 percent trees (forest reserve), grass or herb with or without scattered trees (0 to 5 trees/ha) and open savanna woodland with less than 25 trees/ha.

2 THEORETICAL BACKGROUND

2.1 Construction of a DEM

Topographic data is usually available as isolines, or contours, in either conventional paper map format or in converted digitized forms. In order to use the topographic information together with raster data, it needs to be presented in raster coverages rather than the original lines. The raster surface is acquired through a process of interpolation between the contours.

Global and local methods are the two main groups of interpolation techniques, where the global uses all of the data values and aims at describing a general trend, whereas the local, e.g. splines, uses a limited number of values surrounding a specific point in order to account for small-scale variations. Splines are computionally efficient and create smooth surfaces, while still maintaining the local variation (Eklundh, 1999).

2.1.1 Spline Interpolation

Spline functions can be used to create continuous curves between points in a data set

$$p(x) = b_0 + b_1 x + \ldots + b_k x^k, \quad (1)$$

where p(x) is the actual polynomial, $b_0, b_1, \ldots, b_k$ the coefficients to be determined and k the order of the polynomial (Eklundh, 1999).

Bicubic splines are used when calculations in three dimensions are needed, as for example in a DEM (Burrough & McDonnell, 1998). A spline surface avoids unjustifiable fluctuations by finding the surface with minimum curvature that passes right through the measured values (Dingman, 1993). Bicubic polynoms are here fitted to a limited number of points, and the functions join others in the intersections. The first and second derivatives are continuous which, as a result, produces a smooth surface (Eklundh, 1999).

When processing topographic data, artifacts of natural variation and measurement errors may produce extremely high or low values. The thin plate spline inserts a locally smoothed average instead of the strict spline surface (Burrough & McDonnell, 1998). The smoothing generates an even surface, while still maintaining low residual values between the true points and the thin plate functions. The result is a preserved local variation in the terrain, but also smoothness without abnormalities (Eklundh, 1999).

In a data set, y, that is supposed to contain random errors,

$$y(x_i) = z(x_i) + \varepsilon(x_i), \quad (2)$$

where z is a measurement at a true point, x_i, and where ε is the related random error, the function ought to pass closely to the original data, which gives the spline function, f, that minimizes:

$$A(f) + \sum_{i=1}^{n} w_i^2 \left[f(x_i) - y(x_i) \right]^2 . \quad (3)$$

The first term of *A(f)*, represents the curvature of the spline function *f*, while the second term shows the residuals or error terms. The weight of w_i^2 is inversely proportional to the error variance:

$$w_i^2 = p / Var\left[\varepsilon(x_i)\right], \quad (4)$$

where *p* shows the different user-defined characteristics of the curves and *Var*, the variance (Burrough & McDonnell, 1998).

2.1.2 Hutchinson's ANUDEM

2.1.2.1 Overview

The ANUDEM program is developed by M.F. Hutchinson (1989) at the CRES (Centre for Resource and Environmental Studies) of the Australian National University and has been designed to produce digital elevation models from elevation and streamline data sets (Internet 5). The program is optimized to have the computational efficiency of local interpolation methods, while maintaining the surface continuity of global methods. It is fundamentally a thin plate spline technique, as described above, where the fitted DEM is allowed to follow abrupt changes in the terrain, such as streams and ridges (ESRI, 1997). The technique originates from a minimum curvature interpolation method developed by Briggs in 1974 (Hutchinson, 1989).

The algorithm interpolates elevation data onto a grid through modest smoothing, and at the same time introducing rules that (Hutchinson, 1991):

1. Ensure connectedness in the drainage structure through removal of sinks and pits, and by including a drainage network from stream line data
2. Describe ridges and streams in a proper way through extraction of data from corners of elevation contours

Elevation data will not be radically altered during processing because of the conservative sink removal in the program. Locations in the grid that contradict the input elevation data will be indicated as sinks by the program (ESRI, 1997).

2.1.2.2 Interpolation Algorithm

The iteration works on the basis of a nested grid strategy, which calculates grids at successively finer resolutions. It commences at an initial coarse grid whereafter it halves the pixel size until the user specified resolution is obtained. At each level the data points are placed in the nearest grid point. Grid points in between the allocated data points are calculated using Gauss-Seidel iteration with over-relaxation (Young, 1971; Golub & Van Loan, 1983), while respecting the specified roughness penalty that allow the DEM to follow abrupt changes in the terrain (ESRI, 1997).

The interpolating function, *f*, is defined by the roughness penalty which is made up by the first and second order partial derivatives of *f* :

$$J_1(f) = \int (f_x^2 + f_y^2)\, dx\, dy \qquad (5)$$

and

$$J_2(f) = \int (f_{xx}^2 + 2 f_{xy}^2 + f_{yy}^2)\, dx\, dy, \qquad (6)$$

where the integration range equals the size of the fitted grid. By minimizing $J_1(f)$ over the continuous interpolating functions of *f*, the minimum potential interpolation is obtained and by minimizing $J_2(f)$, minimum curvature interpolation of the thin plate splines is acquired.

A compromise is achieved by minimizing

$$J(f) = 0.5h^{-2}\, J_1(f) + J_2(f) \qquad (7)$$

for all continuous interpolation functions *f* where *h* is the grid spacing (Hutchinson, 1989).

The initial values for the first coarse grid are calculated by using the average height of all data points, while the following finer grid resolutions are based on linear interpolation from the preceding coarser grid (Hutchinson, 1989). When using contours, the algorithm interpolates heights of local maxima based on the surrounding contour height information, since no other information on the maximum height is available (Hutchinson, 1991).

2.1.2.3 Drainage Enforcement Algorithm

It is difficult to handle the occurrence of sinks in a DEM. Manual editing methods are time consuming and subjective whereas the existing automatic methods of smoothing or filtering are efficient at the expense of leveling of well defined surfaces and natural hollows (Mark, 1984). The ANUDEM technique enables the use of drainage enforcement, including the ordered descent and break line conditions that are hidden in streamline data (Hutchinson, 1989).

The drainage algorithm eliminates one of the main weaknesses of elevation grids. It searches for, and tries to remove all sink points that have not been identified as such in the input sink data in order to ensure drainage. A sink will be terminated if it, and its lowest adjacent saddle point, is not associated with an elevation data point. If both sink and saddle are coupled with elevation data, the program makes a decision based on a user-supplied tolerance between drainage enforcement and fidelity to the data. The algorithm follows the same search pattern as the interpolation algorithm, a nested grid strategy, when examining the grid for sinks and saddle points. They are located, however, by comparing the grid point of interest to its eight neighbors, where the value difference between the center cell and the surrounding determines whether it is a sink or not. In order to achieve a linear descent and improving drainage clearance in a grid, ordered chain conditions are applied. This means that each spurious sink

connects via its lowest adjacent saddle point to a data point. The procedure of sink and saddle detection and chain ordering is run once every five Gauss-Seidel iterations.

Three user-supplied tolerances control the behavior of the drainage algorithm. The first tolerance is a measure of the accuracy of the elevation data, in which differences between points have to exceed a supplied threshold value in order to be significant in means of drainage. Points that are clustered at the same height are consequently removed. The second and third tolerances limit the search operations in order to make it as efficient as possible and to prevent drainage clearances from occurring (Hutchinson, 1989).

2.1.2.4 Stream Line Data

When a more accurate placement of the water streams is required, the use of streamline data might be appropriate. The stream line segments can also be used in sink removal where all elevation elements that contradict each down stream flow path are removed, i.e. ordered descent, except for elements that fall under the restrictions set up by the user in the drainage algorithm. The stream lines can also constitute break lines for the interpolation conditions, which in turn ensures that the stream lines are located at their accompanying valley bottoms.

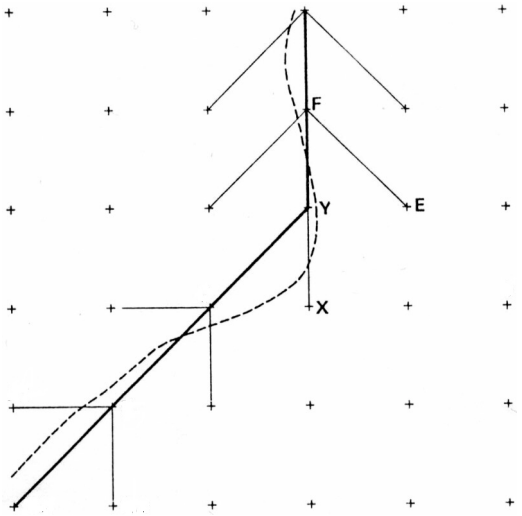

Figure 7. *The streamline network as generalized by straightening of curves in the conditioning procedure of Topogrid. Tributaries are usually at an angle of 45°(the EF segment) to the main channel but can also constitute an extension of the prevailing flow direction, as shown by the XY segment (Hutchinson, 1989).*

The streamline that flows from lower left to the top of the grid in figure 7 (seen as a dashed line) is estimated by straight line segments that are generalized by a change of direction of, at the most 45°, which removes unnecessarily sharp bends in the flow network. Side conditions are usually at an angle of 45° (segment EF in figure 7) to the streamline direction, except at bends, where side conditions can represent the uphill condition (segment XY in figure 7) attached to the lower stream line segment. Each grid point can have several neighboring upper stream segments, but only one down stream segment (Hutchinson, 1989).

2.2 Water Movement in Soils

There are essentially three types of water movement in soils, where the amount of water decides whether it is saturated, unsaturated or by vapor transfer. When all of the pores in a soil are filled with water, the water travels by saturated flow. This occurs below the ground water table, but occasionally also in saturated soils above the water table (Fitzpatrick, 1988). The flow can take place in any direction, and its rate is

depending on the hydraulic conductivity of the soil, determined by the pore size, the pore distribution and the water content. The flow increases as the grains in soils become coarser, i.e. the larger the pores the better ability to lead water (Grip & Rodhe, 1994).

A major part of the flow of water in a saturated soil can be described by Darcy's law (proven by Henri Darcy in 1856) for saturated flow,

$$V_x \equiv \frac{Q}{A_x} = -K_{hx} \frac{d\varphi}{dx}, \tag{8}$$

where V_x [m/s] is the specific discharge which is defined as the volume rate of flow, Q [m^3/s], per unit area, A_x [m^2], at right angles to the x direction. The saturated hydraulic conductivity is expressed as K_{hx} [m/s] of the medium in the x direction, while φ is the mechanical energy per unit mass of fluid. The total potential energy of the fluid is the sum of the elevation above a horizontal plane, z [m], and its pressure head p/γ_w [m] stated as:

$$\varphi = z + \frac{p}{\gamma_w}, \tag{9}$$

where p is the pressure [N/m^2] and γ_w is the weight density of water [N/m^3], which is assumed to be constant in this context (figure 8). Darcy's law describes a flow in a certain direction through a small volume that is large enough to permit averaging of interpore and intrapore variations of velocity. The law applies only to laminar porous-media flows in which flow velocities are low enough for the inertial forces to be negligible. Most natural groundwater flows behave this way, but non-Darcy flow can occur in macropores or in fractures in the soil (Dingman, 1993).

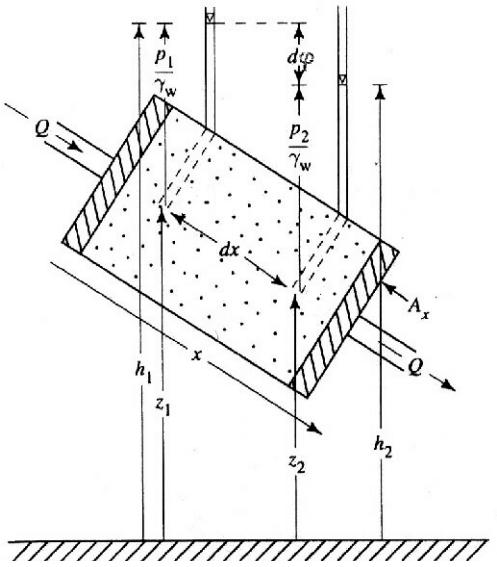

Figure 8. *Variables included in Darcy's law for saturated flow (Dingman, 1993).*

Unsaturated flow takes place when the water in a soil moves over the surface of the grains or aggregates as the pores are partly filled with air. The movement is usually downwards by gravity until field capacity is reached, when lateral and upwards transport arises due to root suction or drying up of the surface. The unsaturated flow process is thus responsible for the equalization of the moisture tension in soils (Fitzpatrick, 1988). The conductivity decreases rapidly as a soil dries out, and the reason is mainly because the large pores, responsible for most of the transport, are emptied first. The unsaturated conductivity is related to the saturated conductivity, its starting point at saturation, but also to the moisture-characteristic curve that defines the amount of available water at a certain pressure (Grip & Rodhe, 1994).

The rate of transport of water by vapor transfer is determined by climatic factors as well as by soil properties. The temperature on the soil surface, partly due to its color, may decide how much of the soil water that will be lost through evaporation, but it also depends on the size and the continuity of the pores in the soil (Fitzpatrick, 1988).

Different soil types allow different kinds of flow; a soil consisting of mainly coarse sand will allow moisture to flow downwards freely, but the flow might change direction as upper layers reach field capacity or become affected by capillarity. In a clay-based soil, on the other hand, the water movement is very slow and the drainage is almost non-existent. The soil loses its moisture chiefly by evaporation, which causes shrinkage of the soil when the particles lose their films of water (Fitzpatrick, 1988).

2.3 Soil Moisture & Topography

Topography is of great importance when it comes to the hydrologic response of a drainage basin to rainfall (Barling et al., 1994). This is due to the control that slope exerts on surface and near surface flow pathways, as well as sub surface flow patterns (Pilesjö et al., 2000). The topographic factors that influence the distribution of soil moisture in a catchment are: 1. Local slope, 2. Specific catchment area, 3. Plan curvature, 4. Profile curvature and 5. Aspect together with topographic shading (Barling et al., 1994).

1. Local slope is a measure of the hydraulic gradient, which is the driving force behind water movements in a catchment
2. Specific catchment area is defined by the local upslope contributing area to any point in a catchment, which means that it determines the potential maximum influx of water to a certain location
3. Plan curvature influences the rate of flow convergence or divergence
4. Profile curvature is a way of describing the rate of change in hydraulic gradient
5. Aspect and topographic shading governs the amount of solar radiation striking a surface and thereby the evapotranspiration in different parts of the terrain

2.3.1 Theory of Topography Dependent Wetness Indices

The use of wetness indices is justified when a simplified, yet realistic, representation of the spatial distribution of soil moisture is desired. The indices can be applied in two different ways. First of all, the cumulative index of a basin can be used to obtain a lumped estimate of the contributing area. Secondly, the index can utilize the spatial soil moisture pattern of a catchment as in this study, which can be used to produce qualitative soil moisture maps. The topographic wetness indices were originally intended for predictions of zones of surface saturation, but their use has been extended to also include predictions of soil moisture patterns (Western et al., 1999).

A large number of topography dependent indices have been developed following the increase in use of digital elevation models (DEMs) and the efficiency in which modern GIS software extracts terrain attributes from these (Barling et al., 1994). The general form of the soil moisture index makes use of local slope and specific catchment area and can be derived from the following theory:

According to Darcy's law, the water flow from one point to another is proportionally related to the total potential difference between the two. This relationship was first intended for saturated flow in the ground, but has also proved its capability of predicting unsaturated flow as well (Grip & Rodhe, 1994).

Studies by Zaslavsky and Rogowski (1969, 1981a) have shown that the permeability of a majority of natural soils decreases with increasing depth and that both unsaturated and saturated lateral flow will develop in these soils provided that the soil layers are at an angle to the horizontal. During a rainfall event, the lateral flow of water will increase the soil moisture content in the down-slope direction.

The following assumptions is inherent in the static topographic soil moisture index (Following Sivapalan, 1987 & Hornberger, 1998):

1. The water table is almost parallel to the soil surface
2. The saturated hydraulic conductivity decreases exponentially with depth
3. Steady state conditions prevail in the catchment and the groundwater recharge rate is uniform

The first assumption means that the subsurface flow, $Q_{subsurface}$ [m^3/s], can be expressed as:

$$Q_{subsurface} = Tc \tan \beta , \qquad (10)$$

where T is the transmissivity of the soil (soil depth multiplied by the hydraulic conductivity of the soil) [m^3/s], c is the contour length [m] and $\tan \beta$ is the slope gradient. The second assumption can be expressed as:

$$K(z) = K_0 e^{-fz}, \qquad (11)$$

where $K(z)$ is the hydraulic conductivity at depth z, K_0 is the hydraulic conductivity at the surface [m/s] and f is a constant describing the rate of change in hydraulic conductivity with depth. In order to calculate the transmissivity of a saturated soil layer with the thickness D (where D is depth to the bedrock and z is depth to the water table), equation (11) is integrated to:

$$T = \frac{K_0}{f}(e^{-fz} - e^{-fD}) . \qquad (12)$$

Due to the fact that e^{-fD} is relatively small in relation to e^{-fz}, equation (12) can be generalized to:

$$T = \frac{K_0}{f} e^{-fz} . \qquad (13)$$

The third assumption suggests that the subsurface flow, $Q_{subsurface}$, can be expressed as a function of drainage area, A [m^2], and recharge rate, R [m/s]:

$$Q_{subsurface} = RA, \tag{14}$$

which means that

$$RA = \frac{K_0}{f} e^{-fz} c \tan\beta \tag{15}$$

$$\Downarrow$$

$$-\frac{1}{f} \ln\left(\frac{RA}{\frac{K_0}{f} c \tan\beta} \right) = z \tag{16}$$

Equation (16) is an expression of the depth to the water table as a function of the topographic variables A and tan β, the soil variables f and K_0 and the climate related variable R. Due to the fact that spatially distributed values of f, K_0 and R are seldom known for an entire catchment area, this reasoning needs further investigation to offer a moisture index independent of the soil and climate related variables. Equation (16) can be simplified as:

$$z = -\frac{1}{f} \ln\left(\frac{Ra}{T_0 \tan\beta} \right), \tag{17}$$

where a is specific catchment area per unit contour length (A/c) and T_0 stands for the transmissivity of the whole profile (K_0/f). Equation 18 expresses the average depth to the water table within the catchment,

$$\bar{z} = \frac{1}{A} \int_{\lambda} z dA = \frac{1}{fA} \int_{\lambda} \left\{ -\ln\left(\frac{Ra}{T_0 \tan\beta} \right) \right\} dA, \tag{18}$$

where A is the total area of the catchment and λ is the mean $ln(a/\tan\beta)$ of the catchment. If equation (17) is used to substitute for R in this equation, the difference between the mean water table depth in the catchment and the water table depth at a specific position can be expressed as:

$$f\left(\bar{z} - z\right) = \left\{ \ln\left(\frac{a}{\tan\beta} \right) - \lambda \right\} - \left(\ln T_0 - \ln T_e \right), \tag{19}$$

where T_e is the average transmissivity of the catchment. $ln(a/\tan\beta)$ in equation (19) is referred to as the topographic wetness index. The spatial variation in transmissivity is often considered unimportant in relation to the topographic wetness index when it comes to the distribution of water in a drainage basin. This means that the relative depth to the water table, WI, can be expressed as:

$$WI = \ln\left(\frac{a}{\tan\beta}\right), \quad (20)$$

where β is the local slope and a [m] is the specific catchment area. The latter is calculated according to

$$a = \frac{A}{c}\ , \quad (21)$$

where A [m^2] is the specific catchment area and c [m] is the contour length. Equation (20) was at first meant to describe the antecedent condition for a rainfall event within the scope of areas where saturation-excess overland flow is most likely to occur. The wetness index is, however, often interpreted as a way of describing long-term moisture conditions in a catchment, where the value of the index increases with increasing soil moisture content up to a level where the index describes areas with permanent saturation.

2.3.2 Non-Steady State Wetness Index

One-dimensional flow of water in soil, referred to as Darcy's law, is given by

$$\frac{Q}{A} = -K \times \frac{d\varphi}{dx} \quad (22)$$

where Q [m^3/s] is the discharge, K [m/s] is the hydraulic conductivity, A [m^2] is the cross-section area and $d\varphi/dx$ [m/m] is the rate of change in hydraulic potential per unit length. The minus sign indicates that the direction of flow is towards decreasing potential in the ground (Grip & Rodhe, 1994). Assuming that the water table is parallel to an impermeable or restricting layer (bedrock), equation (22) can be rewritten as

$$q = K \tan\beta\ , \quad (23)$$

where q is the flux density [m/s] and $\tan\beta$ is the slope of the restricting layer, that in general is considered similar to the slope of the ground surface. Equation (23) is called the kinematic wave equation, which in turn can be used to express the interstitial velocity if the effective porosity of the soil is introduced (Barling, 1996). The effective porosity of soils is a measure of the relation between pore volume and the volume of the solid material (Department of Quaternary Research, 1995). The interstitial velocity of subsurface flow, v [m/s], can be expressed as:

$$v = \frac{q}{\eta} = \frac{K}{\eta} \times \tan\beta\ , \quad (24)$$

where η [m^3/m^3] is the effective porosity of the soil. Iida (1984) used the relationship in equation (24) to develop the idea of time-area curves, which is illustrated in figure 9. The contributing area is dependent on drainage time and continues to expand until the maximum time, t_s, where steady state is reached. When the time reaches t_s, any

point in a drainage basin receives water from all its upstream cells. If the time-area concept is used in calculating specific drainage areas, the resulting wetness index will account for the nature of the topography and the time required to redistribute soil water, which is not the case with the static wetness index. This is of great importance in areas of low relief since the elevation potential in these areas is relatively low. In many situations, the velocity of subsurface flow is very slow, which means that a point is influenced only by a small fraction of its contributing area, and thereby the catchment seldom reaches steady state conditions (Barling, 1996).

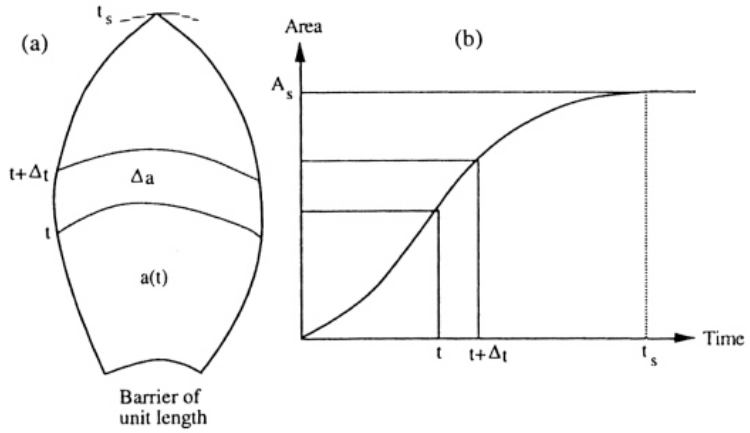

Figure 9. *The time-area concept: (a) The horizontal lines represents isolines of the time required for water to reach the barrier. When the drainage time equals t_s steady state is reached. (b) Time-area curve: the specific drainage area increases until steady state is reached (Barling et al., 1994).*

2.3.3 Flow Direction

When extracting hydrologic information from a DEM, the determination of flow direction from every grid cell is the first step to consider. This is the most critical and at the same time controversial part of hydrological flow modeling (Pilesjö et al., 2000). The most common implementation of this operation in modern GIS software is the one-directional flow algorithm, referred to as the D8-algorithm (D for deterministic). In this implementation a grid cell can drain water to one of its neighboring cells, which is determined by the steepest downhill slope within a 3×3 grid cell window. Every cell in the grid is assigned an integer value indicating the flow direction, e.g. 7=NW, 8=N, 9=NE, 4=W, 6=E, 1=SW, 2=S, 3=SE and 5 indicating sinks in the grid. At every grid cell the algorithm calculates the height difference between the center cell and all of its neighbors. These differences are then multiplied by a distance weight: 1 for N, S, E and W neighbors and $1/\sqrt{2}$ for diagonals, where after the center cell is assigned a drainage direction towards the cell that represents the largest positive difference (Burrough & McDonnell, 1998).

According to Moore (1996) it is possible to achieve a more realistic drainage pattern by replacing the D8-algorithms diagonal distance weights of $1/\sqrt{2}$ with $1/(2-r)$, if r is a randomly distributed variable between 0 and 1. This algorithm, referred to as Rho8 (random), simulates the stochastic behavior of nature, keeping the simplicity of the D8-algorithm (Moore, 1996). The main drawback of the D8 and Rho8 algorithms is its incapability of modeling dispersion (Burrough & McDonnell, 1998). This is considered illogical and could produce severe artifacts if, for example, used in calculation of specific catchment area (Pilesjö et al., 2000).

In order to model flow in a more realistic way a number of multiple-flow direction algorithms have been constructed (Pilesjö et al., 2000). The most common implementation of these algorithms is an approach where the proportion of flow to a downstream cell is calculated on a slope-weighted basis (Freeman 1991 & Quinn 1991). This can be expressed as:

$$f_i = \frac{(\tan \beta_i)^x}{\sum_{j=1}^{8} (\tan \beta_j)^x}, \text{ for all } \beta > 0, \qquad (25)$$

where *i,j* are flow directions (1..8), f_i is flow proportion (0..1) in direction *i*, tan β_i equals the slope gradient between the center cell and the cell in direction *i*, and *x* is a variable exponent (Pilesjö et al., 2000).

The *x* variable in equation (25) determines the amount of dispersion from a cell to its down slope neighboring cells. When *x* approaches infinity this algorithm is comparable to the D8-algorithm and while *x* equals 1 the flow distribution is proportionally related to the slope gradients. It is not however, advisable to apply this algorithm with a constant *x* value, since flow distribution varies depending on location in the terrain. It is common to find less concentrated flow in upper slope areas due to the convex nature of the terrain in these parts, i.e. divergent flow. In the lower parts of the terrain, the often concave slope profile forces the flow into main drainage channels, i.e. convergent flow. Other problems related to estimations of flow distribution are determination of drainage direction over flat surfaces and areas of complex topography. In order to handle these irregularities in the terrain, Pilesjö et al. (1998) constructed a form-based algorithm, Topoform, for calculations of flow distributions. In the case of a convex surface in the DEM, the flow is distributed to all grid cells with lower elevation values, whereas in the case of a concave surface the flow is directed in the main drainage direction (Pilesjö et al., 2000)

2.4 The Influence of Soil & Vegetation Properties on Soil Moisture

2.4.1 Soil Properties

The ground consists of solid materials, liquids and gas. The solids are the foundation that decides the size of the pores that are filled with liquids and gas. The soil porosity is defined as the proportion of the pore volume in the total soil volume. The porosity varies between 28 and 48 percent for spherical mineral grains depending on the degree of packing. A mineral soil shows a porosity of around 30 – 60 percent, while the corresponding value for peat is 90 percent (Grip & Rodhe, 1994).

The soil texture is usually said to be the distribution of the pore size in a soil, but there is a difference between coarse-grained soils and fine grained ones. The small grains in the finer soils tend to build larger aggregates, in between which larger pores appear (Grip & Rodhe, 1994). Some aggregates can be very stable, as for example in Ferralsols, where ploughing can be done right after heavy rains since the high content of iron makes the aggregates very resistant, and hence water drainage is facilitated. (Fitzpatrick, 1988). This, the soil structure, can be found in the upper layers of a soil because of biological or agricultural activity, resulting in a grainy consistence despite

its fine components. A way of improving the soil properties in agricultural practices is to increase the soil structure, which improves the development of a crop (Grip & Rodhe, 1994). Macropores occur in soils as cracks or in former root passages and influences the transport of water (Fitzpatrick, 1988).

The distribution of soil moisture is largely controlled by variations in various soil properties, such as texture, organic matter content, structure and macroporosity, all of which affect the water transmission and retention in the soil (Famiglietti et al., 1998).

The proportion of water in a soil sample is expressed as the water content in units of volume percent. Saturation occurs when all of the pores are filled with water, which equals the volume of soil porosity. As depth increases and when entering the saturated zone below the ground water surface, the pressure is greater than the atmospheric. Above this level, in the unsaturated zone, the pressure decreases to a lower level than that of the atmosphere. The ground water level is the level where the water pressure corresponds to the atmospheric equivalent (Grip & Rodhe, 1994).

Most of the available soil moisture comes from precipitation, of which the major part is lost through drainage or by evapotranspiration. Light rain is easily absorbed by a bare soil, whereas heavy showers cause accumulation and associated run-off at the soil surface, which may result in erosion. During rainfall, water usually moves downwards through the soil, but the moisture can move in the opposite direction due to capillarity when the surface layers are drying out (Fitzpatrick, 1988).

The soil water is held around soil particles with different degrees of suction. At the moment of exposure to water, the soil aggregates absorb the liquid and distribute it between the grains until a thin film, i.e. a state of equilibrium, is reached. Excessive water is drained away, and the saturated soil is said to be at field capacity. Plants will continue to absorb water out of the soil until the wilting point is reached (Fitzpatrick, 1988). It is the water content during drying that causes the plant water uptake to cease (Grip & Rodhe, 1994). Thus, the water between the field capacity and the wilting point is considered being plant available water (Fitzpatrick, 1988). The finer the grains (or pores) in the soil, the greater the water content at field capacity (figure 10) (Grip & Rodhe, 1994). Clay based soils usually hold significant amounts of water, but most of the available moisture is also below the wilting point (Fitzpatrick, 1988).

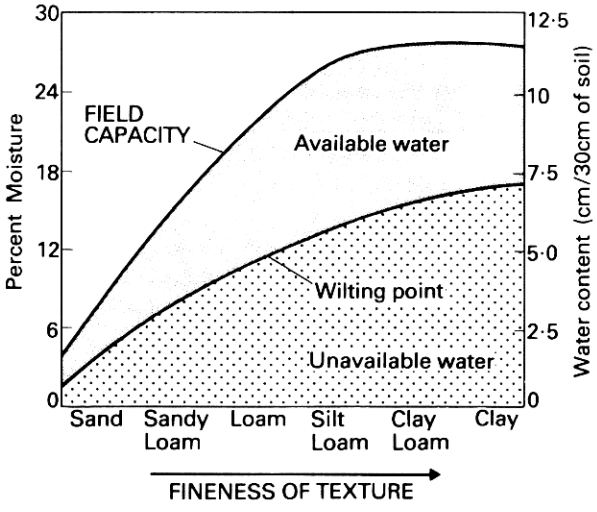

Figure 10. *Plant available water as determined by field capacity and wilting point, depending on the fineness of the texture of soils (Fitzpatrick, 1988).*

2.4.2 Vegetation Properties

The soil moisture variability is influenced by different vegetation properties through their water distributing abilities. The canopy of trees prevents moisture from reaching the ground through interception and thus evaporation. The foliage also shades the ground surface, which changes the evaporative properties of the soil, while the structure of the vegetation also gives rise to turbulence that affects the evapotranspirative properties of the soil-vegetation system. The hydraulic conductivity of the soil is changed by organic material deposition, i.e. plant litter, on the soil surface (Famiglietti et al., 1998). It can also fluctuate through the influence of roots, which are important for their transporting properties. They create a negative pressure, typically around 150 meters, in order to absorb the water bound in the soil. The root zone is where the distribution downwards (to the ground water) and upwards (through plant uptake), of the precipitation takes place (Grip & Rodhe, 1994). The rate of influence of these factors on soil moisture depends on the vegetation type, density and season (Famiglietti et al., 1998).

3 MATERIAL

- *Topographic paper maps*
  Paper maps were used in planning of the fieldwork as well as for navigation in the area. They are based on aerial photographs gathered in 1960 by the Ghanaian Survey Department, and include topographic contours with an equidistance of 15 meters. The projection is Transverse Mercator applied on the Ghana National Grid in a 1:50 000 scale.

- *Digital topographic contour data*
  These data, with a contour interval of 15 meters based on the mentioned topographic paper maps, was acquired from the Ghanaian Survey Department for the region of interest. The projection is Transverse Mercator applied on the Ghana National Grid.

- *Digital hydrographic data*
  The data was attached to the topographic contour material and represents the regional drainage network as presented on the paper maps.

- *Digital soil map*
  The soil map for the study area is produced by the Soil Research Institute (CSIR) in Ghana and is classified according to the Ghanaian soil classification system. It is digitized from a 1:500 000 paper soil map of the Upper East Region, referenced according to the Ghana National Grid.

- *Digital geological map*
  Information on the geology was included in the soil data set.

- *Country At a Glance CD-ROM*
  The disc is produced by the Environmental Protection Agency (EPA) in Ghana in cooperation with the World Bank in 1999. It is available as an interactive database in the Ghana National Grid as well as in Lat Long. The information below was used as reference material:
    - Digital vegetation map, generalized from a vegetation map based on interpretation of TM satellite data as of 1994
    - Digital information on the location of roads, communities and other features, generalized from an updated road mapping during 1994, based on older maps, TM satellite data and GPS tracking

- *Collected Field Data*
    - GPS recordings
    - Soil data
        - Soil water content
        - Soil texture, as primary and secondary fractions
    - Vegetation and land use data
    - Topographic evaluation data

4 METHODOLOGY

4.1 Field Measurements

Field measurements were conducted in the Tamne River Basin starting on October 13 and ending on October 27, 1999. Road sampling was applied in the vast area since an even distribution of the data was desired, as well as representation of different topographic settings (Appendix 4). Figure 11 illustrates the position of the 7 transects. The A, B, C, E and H transects (the D transect was removed since no useful data was acquired) have sample point intervals of approximately 1 kilometer, whereas the F and G transects have a denser distribution of about 100 meters. The transects are positioned parallel to the roads at an estimated distance of 50 meters, to reduce the effect of drainage disturbances. The effect of the roads is most likely small, since they are constructed through leveling of the natural foundation.

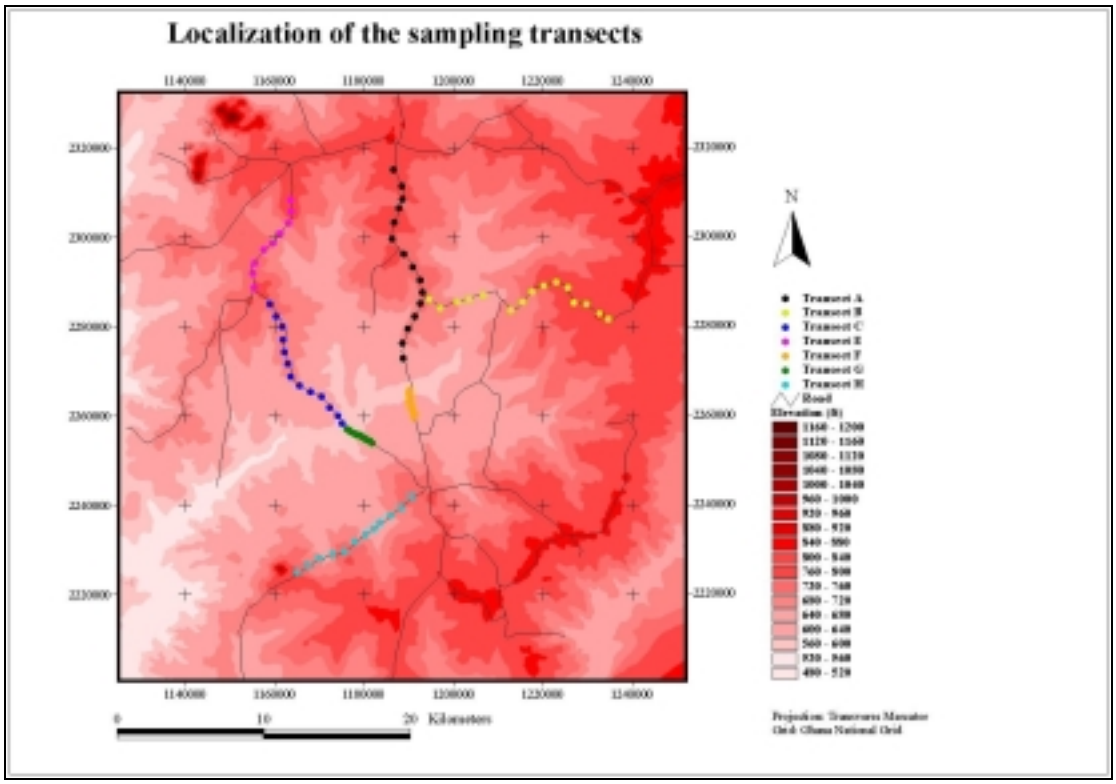

Figure 11. *The transect locations along roads in the study area. All transects are sampled at a point equidistance of approximately 1 km, except for the F and G transects that have a corresponding interval of 100 m.*

At each point location, a special instrument was used to collect the soil sample at the desired depth of 25 - 35 centimeters. This level was chosen since roots usually are concentrated in the upper 50 centimeters of the soil (Grip & Rodhe, 1994). The instrument is used as a drill, working its way down in the soil by manual twisting, during which time soil progressively is collected in a container. The tool is constructed in a way that makes the sample procedure uniform, which is why the

samples always represent a consistent interval in the soil profiles. After the collecting, the specimens were put in plastic bags and sealed to preserve the moisture content, before weighing and drying in the laboratory.

In addition to the soil samples, representative photographs were taken and a number of parameters estimated by visual inspection: type of vegetation, land use, vegetation cover [%] and vegetation height [m]. The location of each sample point was recorded three times using the GPS (Magellan NAV DX 10): when arriving at the point, before leaving the point and once in between. The GPS-position finally used was the median of these three recordings. This method was applied in order to get a position as accurate as possible, considering the time available at each point.

In order to extract the soil moisture content in each soil sample the gravimetric method was used (Department of Quaternary Research, 1995). The samples were weighed (using a Mettler PM 200 precision scale) and then dried for 24 hours at 105°C (in a Gallenkamp Hotbox Oven, Size 2), whereafter the dry weight was measured. The difference between the wet and dry weight represents the prevailing moisture in the samples, which was used in the following formula to assess the moisture status of each sample:

$$SM = \frac{wm}{sdm}, \tag{26}$$

where *SM* [%] is the soil moisture content, *wm* [g], the weight of the water and *sdm* [g], the dry weight of the soil.

While analyzing the wet and dry weights of the soil samples, a rough estimation of the two dominating soil fractions was made. This method, by manually examining the soil, resulted in a Soil Texture Index (STI) consisting of a primary and secondary fraction. The different combinations were given an index number, 1 – 9, which could later be compared with the soil moisture (table 1). As the value of STI increases, the water holding capacity of the soil increases.

Table 1. *Manual interpretation of soil texture, resulting in a Soil Texture Index (STI). Fraction 1 is the dominating fraction in each sample, whereas Fraction 2 is considered being less significant.*

Fraction 1	Fraction 2	STI
Gravel	Gravel	1
Gravel	Sand	2
Gravel	Clay	3
Sand	Gravel	4
Sand	Sand	5
Sand	Clay	6
Clay	Gravel	7
Clay	Sand	8
Clay	Clay	9

The vegetation at the sample points was also quantified as an index. The height [m] multiplied by the vegetation cover [%] of plants or crops resulted in a measure of the

prevailing biomass at each location. Both of the parameters were gathered using sound estimations in order to achieve a local average.

4.2 Correction of the GPS Recordings

The position of the sample points was measured using the WGS 84 map datum and the lat/long coordinate system. In order to make these points compatible with data referenced according to the Ghana National Grid, they were transformed using the Project module in Arc/Info. Due to a spurious relationship between the global coordinate system (WGS 84) and the Ghana National Grid, the result of this transformation required some correction.

In Ghana GPS-data were recorded during half an hour at two triangulation points (information on which was acquired from the Ghanaian Survey Department), located approximately 30 kilometers west of Bawku. The position was stored every minute and finally a mean value of the measurements was calculated. These mean values were transformed from the global to the local coordinate system and compared to the "real" positions of the triangulation points. The mean error of the discrepancy between the "true" positions of the triangulation points and the GPS recordings for the same point, was 29 meters in the X direction and 357 meters in the Y direction. In other words, the positions of the sample points were displaced towards the northeast, most likely due to inaccuracies in the description of the relationship between the global coordinate system and the Ghana National Grid. Furthermore, inaccuracies of the GPS receiver might have contributed to these errors. According to this fact, 29 meters was subtracted from the X coordinate of all sample points and 357 meters was subtracted from the Y coordinate of all sample points. After this affine transformation, the positions of the sample points seemed to coincide with the true sample locations. This was verified by the consequent placement of points at the proper side of the roads, as well as sample points taken on bridges being properly located at the intersection of roads and water streams.

4.3 Construction of the DEM

The original material used when constructing the DEM was acquired from the Ghanaian Survey Department as topographic contour lines and water streamlines in ARC/INFO format (.e00-files). The files were imported and appended in ARC/INFO, in order to suit the area of interest, i.e. the Tamne River Basin.

Since the drainage network in the basin had to behave in a topologically correct manner prior to the drainage-imposed interpolation, the water stream arcs were examined for drainage direction. The procedure requires that all arcs are pointing downslope and that there are no braided streams or polygons in the network. The arcs were turned into the downslope direction by both automatic flipping and manual measures, where the automatic function was not sufficient. Braided streams and spurious polygons were removed by manual editing. The interpolation was then performed in the ARC/INFO Topogrid module, based on the ANUDEM program as described in section 2.1.2, to produce a DEM with a resolution of 50 meters.

When interpolating in Topogrid, the only tolerance that was modified, following the recommendations (equation 7), was the {tol1} that reflects the accuracy and density of the elevation points. Data points that block drainage by no more than this tolerance are removed. When using contour data this should be set to half of the contour interval (7.5 meters). The default values for the two remaining tolerances have been found to be very robust (ESRI, 1997) and consequently they were left unchanged.

The Fill command in Arc/Info adjusted for the spurious sinks found after the initial processing of the topographic material. The conditioned DEM was then considered valid and further calculations could be conducted.

4.4 Evaluation of the DEM

Information regarding local topography was gathered during the fieldwork for the evaluation of the previously constructed DEM. These data include measurements of two different slope profiles, of which the first is located next to the SARI Manga station and the second is a hill formation a few kilometers west of Garu Natinga. The SARI profile was chosen since it represents the typical slope properties in the Tamne River Basin, while the second profile is one of the few topographic features in the basin that show steep slopes.

The acquisition of slope data was done by manual measuring of slope angles over distances of 50 meters. The latter were measured using a metal measuring tape, while the slope angle of each segment was estimated with a clinometer, where the angle accuracy was estimated at 1/4°.

The length of the SARI Manga profile is 1200 meters, i.e. 23 points with equidistance of 50 meters, whereas the corresponding profile at the hill formation consists of 9 points distributed over 400 meters. The angle and segment length data were used when computing the elevation difference between the profile measurement points, as the height difference between the corresponding locations in the DEM could then be evaluated.

4.5 Calculations of Topographic Attributes

4.5.1 Calculations of Slope & Aspect

The slope DTM was produced from the DEM in ArcView through the command Derive Slope, where the rate of maximum change for each cell to its neighbor (a 3×3 pixel window) is calculated. This produces a grid in which each cell contains a continuous slope value represented in degrees. Each cell in the aspect theme, also produced in ArcView, represents the direction that the slope faces, as defined by a 3 by 3 pixel window around the cell. The aspect values are continuous, starting at 0 degrees (north) and increasing clockwise until 360 degrees is reached at north again (ESRI, 1997).

4.5.2 Calculation of Wetness Index Based on One-Directional Flow

In order to calculate a wetness index based on one-directional flow of water over the DEM, the Flowdirection module in Arc/Info was used to establish the drainage

network. This module is a simple D8-algorithm as described in the theory section. The output from this procedure was then used in the Flowaccumulation module of Arc/Info, which traces the flow of water upstream from every grid cell, in order to calculate its specific catchment area. The generated specific catchment area grid was then reclassed to include only those values below the CIT-limit (Channel Initiation Threshold), which was determined through trial-and-error. A CIT-value of 100 pixels, which corresponds to 50 000 m^2, created a drainage network resembling the mapped drainage network (figure 12).

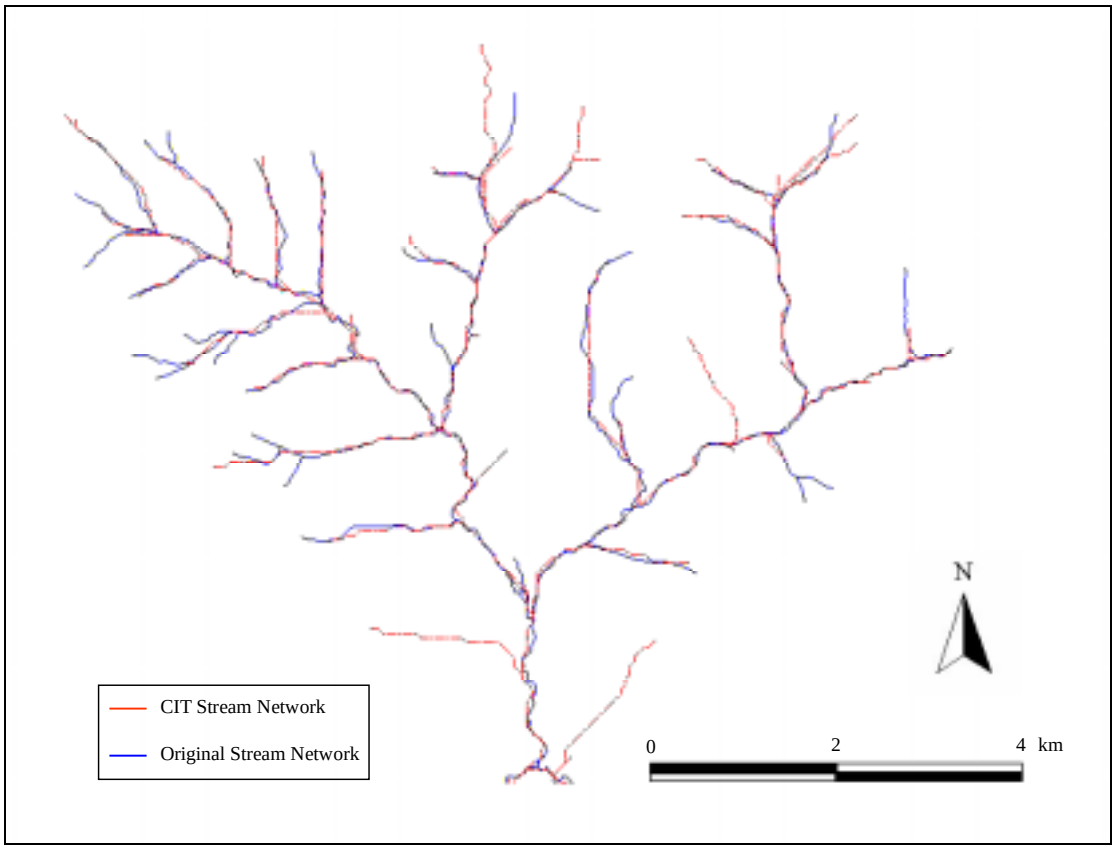

Figure 12. *Stream network, created by specifying a Channel Initiation Threshold of 100 pixels in the flow accumulation grid (red color), superimposed on the original stream network (blue color).*

The reclassed flow accumulation grid and the derived slope data layer were then used in simple map algebra to create a wetness index grid, according to:

$$WI = \ln\left(\frac{a_o}{\tan\beta}\right). \qquad (27)$$

WI is the topographic wetness index, a_o [m] specific catchment area based on one-directional flow divided by the contour length of 25 meters, and β, the local slope.

4.5.3 Calculation of Wetness Index Based on Multi-Directional Flow

In order to calculate a wetness index based on multi-directional flow of water over the DEM, the Topoform program (Pilesjö et al., 2000) was used in order to establish the drainage network. The algorithm of this program is described in section 2.3.3. The

output from Topoform consists of eight grids, preferably named n, s, w, e, nw, ne, sw and se, indicating the fraction (0-100) of each cell draining in a specific direction. For example, if the s-grid at position 2,2 has a value of 30, then 30 percent of its specific drainage area is distributed towards the south.

In order to derive the specific drainage area from the established drainage network, an application called SteadyIndex was created in Visual Basic 6. This application traces the upstream flow network from every grid cell in a recursive process (using the output from Topoform) in the following way:

1. The grid cell under examination is assigned the value true

2. Recursive procedure: Trace
    a. If the current cell receives drainage from its northern neighbor &
       If the current cell does not drain towards the north &
       If the value of the northern neighbor is false &
       If the contribution from the northern cell hasn't been calculated
       Then
            The northern neighbor is assigned the value true
            The Trace procedure is called with the position of the northern draining cell as input parameters
            When returning from the recursive call the northern cell is assigned the value of the area received from its neighbors multiplied by the percentage it distributes towards the south
            The northern neighbor is set to false.
    b. Same procedure as in case 2a applied to the northeastern neighbor of the current cell.
    c. Same procedure as in case 2a applied to the eastern neighbor of the current cell.
    d. Same procedure as in case 2a applied to the southeastern neighbor of the current cell.
    e. Same procedure as in case 2a applied to the southern neighbor of the current cell.
    f. Same procedure as in case 2a applied to the southwestern neighbor of the current cell.
    g. Same procedure as in case 2a applied to the western neighbor of the current cell.
    h. Same procedure as in case 2a applied to the northwestern neighbor of the current cell.

3. The cell under examination is assigned the area it receives from its neighboring cells and false.

These three steps are applied on all grid cells starting at position 1,1 and ending at nrows, ncols (number of rows and columns in the DEM). The output from SteadyIndex is an Idrisi image raster file (ASCII-format) containing the specific drainage area of each cell in the grid. The assignment of a Boolean data type (true/false) to the grid cells when tracing the flow is done in order to avoid the case when the Topoform program had produced a circular drainage network (a cell receives drainage from itself). By checking whether a cell already has been visited or

not, the application is prevented from going into an eternal loop. Appendix 3 shows the source code for the main algorithm of the application.

The generated specific catchment area grid produced by the SteadyIndex application was then reclassed in the same way as in the case of specific catchment area based on one-directional flow, i.e. the CIT value was set to 100 pixels. Since the specific catchment area used in calculations of the wetness index is defined as a specific catchment area divided by the contour length, the eight files produced by the Topoform application were reclassed so that all cells in each grid containing a value separated from zero was assigned a value of one. These eight images were then used in an overlay operation (addition) to form a single grid containing the number of cells each cell distributes water to. This grid was then used together with the specific drainage area grid and the slope grid, to produce a wetness index according to:

$$WI = \ln\left(\frac{a_m}{\tan\beta}\right), \tag{28}$$

where WI is the topographic wetness index, a_m [m], the specific catchment area divided by the contour length (in this case one neighboring cell represented 25 meters) and β, the local slope.

In order to account for possible position errors in the GPS measurements of the sample points, a map containing filtered wetness index values was created. The purpose of filtering, or averaging, is the possibility to find a representative value for the point in question. This might also, however, result in deterioration of the data quality since filtering of the wetness index values results in lower differences between neighboring pixels. In this operation, an average filter with a search window of 3×3 pixels was used.

4.5.4 Calculation of Wetness Index Based on Multi-Directional Flow, "Non Steady State"

In order to calculate a wetness index based on multi-directional flow that also incorporates the time required for water to be distributed in the terrain, an application called NonSteadyIndex was created in Visual Basic 6. This application uses the same input as the SteadyIndex application, i.e. the output from Topoform, and produces a text file containing the specific drainage area of transect sample points (dependent on a user specified drainage time).

The first step of the algorithm involves finding the spatial extent of the specific drainage area, given the user specified drainage time. In order to do this, an additional data layer is used, where the value of each grid cell constitutes the drainage time for that particular cell (the time required for water to pass a grid cell). However, the drainage time is more like a relative time index, since it is only based on local slope. The varying soil properties of the study area were not known, which led to this simplification.

In order to find the spatial extent of the specific drainage area, a recursive procedure traces the flow in the drainage network until the cumulative drainage index equals the user specified drainage index. Whenever the algorithm passes a grid cell, that cell is

assigned “true” in a Boolean data layer. In the next step a modified version of the trace procedure, from the SteadyIndex application, is used to calculate the specific drainage area. This modified procedure calculates the area of the grid cells that were set to true during the first step.

Since there was no spatial data concerning saturated hydraulic conductivity and effective porosity available, the application was run with five relative drainage times. These runs covered the range from zero contribution from neighboring cells to almost steady state conditions. The generated specific drainage areas were then used in the same manner as in the case of the steady state index (described above), to produce the wetness index. Appendix 3 shows the source code for the main algorithm of the application.

4.6 Statistical Analysis

4.6.1 Correlation Analysis

When analyzing the compiled data material (figure 13) in searching for a statistical model explaining the distribution of soil moisture, a correlation matrix (Pearson correlation coefficient) was constructed for each transect and for the data set including all points. This information is vital when sorting out suitable predictor variables for the regression analysis as much as finding intercorrelated variables to be considered in the analysis. Intercorrelation, referred to as multicollinearity, exists when two predictor variables are highly correlated to each other, which may cause problems since the variables explain the same variability in the response variable.

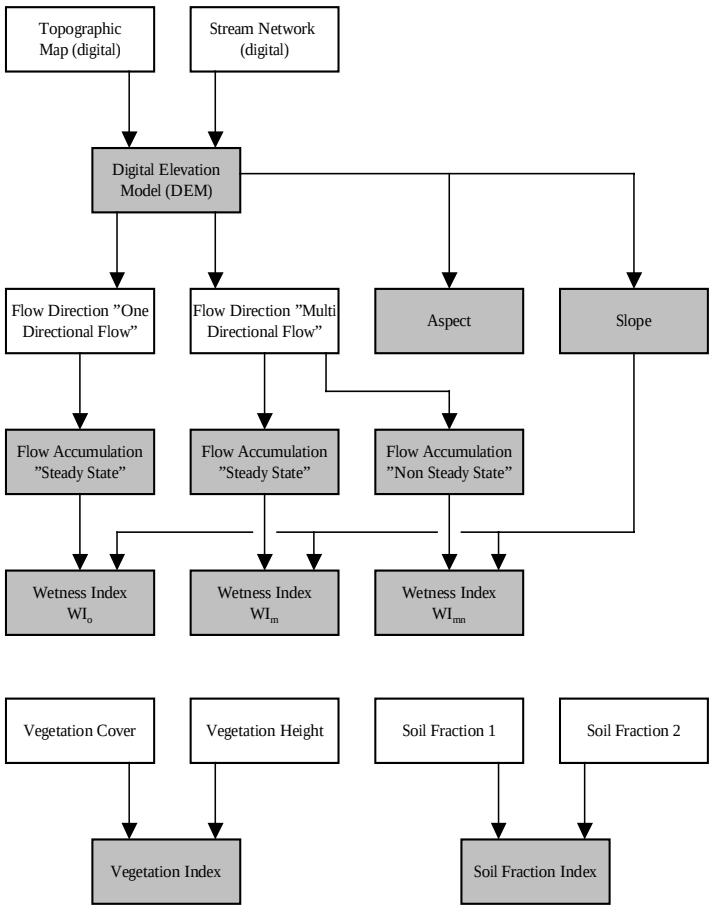

Figure 13. *Input sources and data derived from these. Grey boxes indicate variables included in the statistical analysis.*

The significance of each correlation between the predictor variables and the response variable (soil moisture) was tested using the 0.10 significance level in a table describing critical values of the Pearson product-moment correlation coefficient. Even though this method is not complete in terms of finding "real" relationships between variables, it rules out the most unlikely ones. Relationships having a correlation coefficient above and slightly below the critical limit, were used in the following regression analysis.

4.6.2 Regression Analysis

The determination of the significance of the ratio of explained to unexplained variance, F-statistics, is important in considerations of effectiveness of a regression model in accounting for the variability of the response variable. The null hypothesis of an F-test is that of no explanation of the variability of Y in terms of X. H_0 is rejected if the computed F-value exceeds a critical F-value, and thus the predictor variable can be used to make reliable estimates of the dependent variable (Shaw & Wheeler, 1996).

In order to find suitable statistical models for estimation of the soil moisture distribution, stepwise regression analysis was carried out in Minitab. This method is useful when trying to find the best subset of predictors. Minitab offers three different kinds of procedures within this context: standard stepwise regression, forward selection and backward elimination. In this case standard stepwise regression was applied on all of the individual transects, as well as on the complete data material. This procedure works in the following way: First, F-statistics for predictors already included in the model are calculated. If any of these have a value less than the user-specified parameter "F to remove", the predictor with the smallest F-value is excluded from the model. Secondly, F-statistics for predictors not yet included in the model are calculated. If any of these have a value larger than the user specified parameter "F to enter", the predictor with the largest F-value is included in the model. If no additional predictors can enter the model, the process is terminated. The user defined parameters "F to remove" and "F to include", were both given a value of 4. The stepwise regression procedure generates t-statistics for the individual predictors in the regression equation. This measure is simply the square root of the F-statistics (Minitab Inc., 1998).

When performing regression analysis it is important to analyze the residuals of the resulting regression equations. In order to produce a reliable regression equation, the residuals should be normally distributed around the regression line, and the degree of scatter around the regression line should not vary. These requirements mean that the residuals should have zero mean and unit variance over the complete range of observed independent terms (Shaw & Wheeler, 1996). These prerequisites were checked by visually inspecting residuals plots for the regression equations.

To test if autocorrelation in the regression residuals exists, a Durbin-Watson test was applied on each regression equation. In order to accept or reject the H_0 hypothesis of absence of autocorrelation, the resulting D value was compared to table values of critical bounds at the 0.05 significance level.

5 RESULTS

5.1 Correlation Analysis

Table 2 shows the Pearson correlation coefficient for relationships between selected predictor variables and the soil moisture (SM). The Soil Texture Index (STI) is the only independent variable that shows a significant correlation when examining the complete data series, and during analysis of all the separate transects. Other variables that repeatedly show a significant relationship with the soil moisture are the wetness index based on multi-directional flow (WImulti) and its filtered counterpart (WImultif). The wetness index based on one-directional flow, the wetness index based on multi-directional flow (non steady state conditions), slope, aspect and elevation never show a significant correlation with soil moisture. The G transect is worth noting, where both the filtered and the unfiltered specific drainage areas (MultiA and MultiAf) show strong correlations with SM. However, when introducing the slope and the contour length in calculating the wetness indices (WImulti and WImultif), the correlation coefficient is reduced.

Table 2. *Pearson correlation coefficient for selected predictors. The critical correlation values is estimated at the 0.10 significance level for N samples. In the case of the complete data material, only the relationship between SM and STI is considered significant, even though the critical correlation value permits other variables (exceeding a value of 0.170) to be analyzed further. Bold figures represent the best correlation within each predictor.*

Predictor	*A*	*B*	*C*	*E*	*F*	*G*	*H*	*All data*
N	15	15	12	9	15	15	13	94
Critical Value	0.441	0.441	0.476	0.582	0.441	0.441	0.497	0.170
STI	0.764	0.582	0.787	0.667	0.830	0.726	**0.916**	0.745
MultiA	0.421	-0.114	0.405	-0.273	-0.004	**0.636**	-0.027	0.122
MultiA/c	**0.427**	-0.066	0.405	0.112	-0.116	0.387	0.109	0.175
WImulti	0.457	-0.112	0.539	0.377	-0.182	**0.504**	0.093	0.138
MultiAf	0.346	-0.053	0.443	**0.748**	0.040	0.728	0.153	0.259
MultiAf/c	0.377	-0.016	0.426	**0.800**	-0.128	0.521	0.279	0.300
WImultif	0.417	-0.093	0.589	**0.893**	-0.230	0.560	0.280	0.249
VegCov	-0.265	0.334	0.448	0.021	0.452	0.013	**0.548**	0.336

Table 3 illustrates the Pearson correlation coefficient for intercorrelations between STI and WImulti or WImultif. In cases where the correlation analysis indicates a relationship between SM and WImulti or WImultif, the intercorrelations are weak to moderate. The strongest intercorrelations are found between STI and WImultif for the C and E transects.

Table 3. *Intercorrelations between STI & WImulti or WImultif*

Predictors	*A*	*B*	*C*	*E*	*F*	*G*	*H*
STI & WImulti	0.406	-0.519	0.562	0.219	-0.092	0.236	0.154
STI & WImultif	0.412	-0.521	0.649	0.635	-0.125	0.308	0.304

5.2 Regression Analysis

5.2.1 Transect A

The topography of the A transect (15 samples) ranges from 200 to 246 meters and constitutes an almost uniform slope profile with a continuous drop in elevation, when moving from north to south (Appendix 4). The slope of each individual sample point ranges from 0.15° to 1.58° with an average value of 0.56°. The land use is dominated by agriculture but there are some elements of pasture present. The soil moisture content, according to the lab analysis of the soil samples, ranges from 6 to 12 percent with an average value of approximately 9 percent. The Soil Texture Index (STI) shows that no specific texture class dominates among the samples.

The result from a stepwise regression analysis and Durbin-Watson statistic, using STI, MultiA, MultiA/c, WImulti, MultiAf, MultiAf/c and WImultif, is presented in table 4. The best subset of predictors in this case constitutes the model where only STI is included, which explains 58.4 percent of the variability in soil moisture. The remaining predictors where excluded due to their incapability of explaining the variability in soil moisture (F-value being lower than the allowed limit). Figure 14 shows STI plotted against SM.

Table 4. *Regression equation and statistical measures for the A transect.*

Regression Equation	R^2	T-value	D
SM=0.0364+0.00895STI	58.4	4.27	2.13

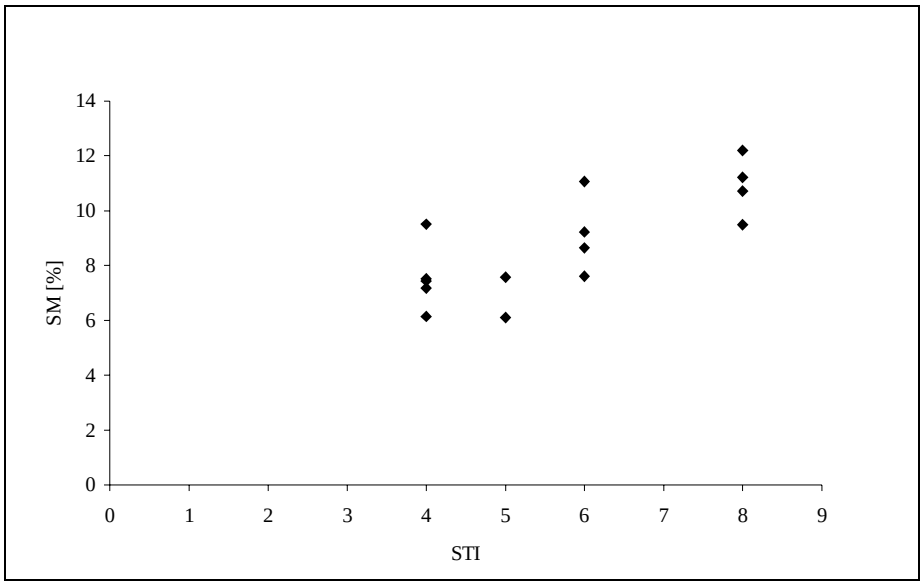

Figure 14. *Soil moisture plotted against the Soil Texture Index, STI, for the A transect.*

Through the study of residual plots for the regression equation, it can be concluded that the residuals are not ideally distributed. Given critical bounds of the Durbin-Watson statistic at the 0.05 significance level and D for the regression equation the hypothesis of autocorrelation in regression residuals can be rejected.

5.2.2 Transect B

The topography of the B transect (15 samples) ranges from 194 to 260 meters. In this case, however, the samples are not taken along a homogeneous slope but along a section of rather varying topography in an east-westerly direction (Appendix 4). The slope of each sample point ranges from 0.09 to 1.7°, with an average value of 0.75°. No specific texture class dominates in the area, where the most widespread land use is agriculture. The soil moisture varies from 6 to 18 percent with an average value of 10 percent.

The result from a stepwise regression analysis and Durbin-Watson statistic, using STI and VegCov, is presented in table 5. The best subset of predictors constitutes the model where only STI is included, which explains 33.8 percent of the variability in soil moisture. Figure 15 shows STI plotted against SM.

Table 5. *Regression equation and statistical measures for the B transect.*

Regression Equation	R^2	T-value	D
SM = 0.0427 + 0.0107STI	33.8	2.58	2.53

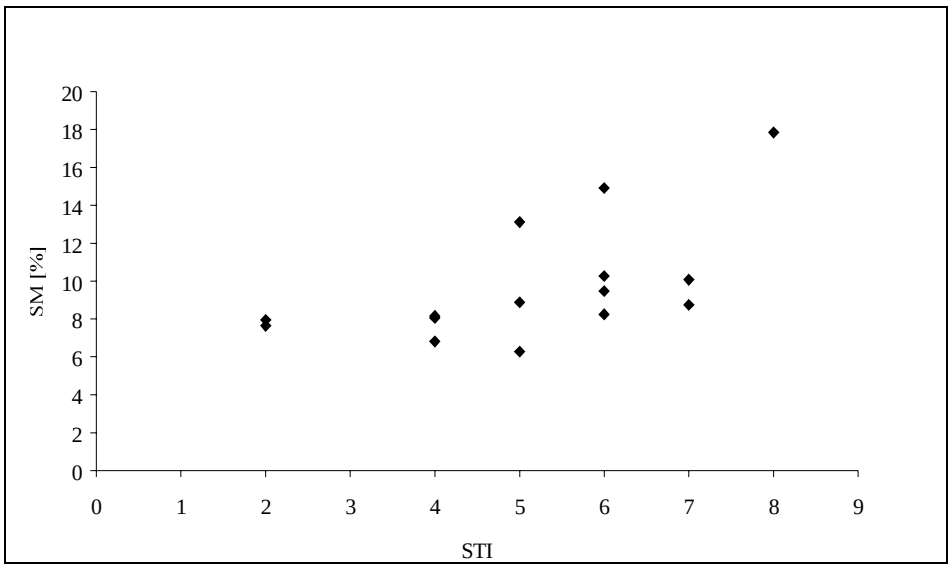

Figure 15. *Soil moisture plotted against the Soil Texture Index, STI, for the B transect.*

By studying the residual plots for the regression equation, it can be concluded that the preferred normal distribution of residuals is absent. The Durbin-Watson statistic shows that the hypothesis of autocorrelation in the regression residuals can be rejected.

5.2.3 Transect C

The topography of the C transect (13 samples) ranges from 175 to 227 meters, along a fairly homogeneous slope, in a north-west south-easterly direction (Appendix 4). The slope of the individual sample points varies between 0.09 and 0.97°, with an average value of 0.44°. The STI indicates that "4" constitutes the main texture class in the area, which is mostly used as pasture. The soil moisture content ranges from 7 to 15 percent with an average value of 10 percent.

The result from a stepwise regression analysis, using STI, MultiA, MultiA/c, WImulti, MultiAf, MultiAf/c and WImultif, is presented in table 6. The best subset of predictors constitutes the model where only STI is included, which explains 61.9 percent of the variability in soil moisture. Non of the topography dependent predictors, nor the VegCov, have F-ratios large enough to be included in the model. Figure 16 shows STI plotted against SM. Through the study of residuals plots for the regression equation it can be concluded that regression residuals are far from being normally distributed. A Durbin-Watson statistic is not available for this transect, since the number of samples is too low.

Table 6. *Regression equation and statistical measures for the C transect.*

Regression Equation	R^2	T-value
SM=0.0504+0.0102STI	61.9	4.23

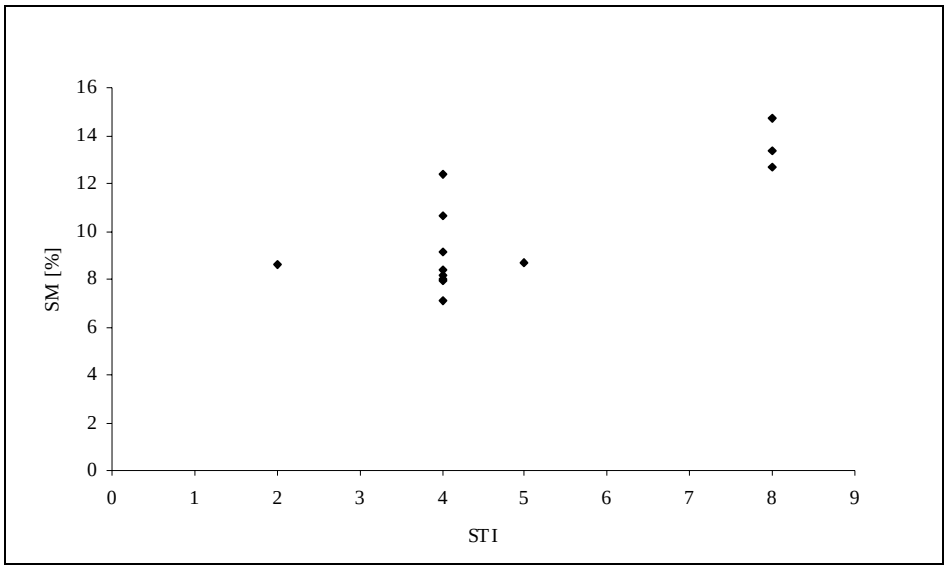

Figure 16. *Soil moisture plotted against the Soil Texture Index, STI, for the C transect.*

5.2.4 Transect E

The topography of the E transect (9 samples) ranges from 210 to 245 meters, along a stretch of undulating terrain in a north-east south-westerly direction (appendix 4). The slope varies between 0.12 and 2.4°, with an average value of 1.04°. The main type of land use is agriculture. It is worth noting, however, that 2 sample points are located within a forest reserve, where the vegetation differs from that of the surrounding areas. The soil moisture content ranges from 4 to 18 percent, with an average value of 9 percent. The STI values of the sample points do not indicate any specific texture class being over-represented.

Table 7 summarizes the result from a stepwise regression analysis using STI, WImulti, MultiAf, MultiAf/c and WImultif. The best statistical model for the E-transect is the one using only WImultif as predictor, which explains 79.8 percent of the variability in soil moisture. The incorporation of other variables in the model was

not allowed, since the individual F-ratios of the remaining predictors were too low. Figure 17 shows STI plotted against WImultif. A Durbin-Watson statistic is not available for this transect, since the number of samples is too low. Through the study of residual plots for the equation, it can be concluded that the regression residuals are far from being normally distributed.

Table 7. *Regression equation and statistical measures for the E transect.*

Regression Equation	R^2	T-value
SM=-0.255+0.0377WImultif	79.8	5.26

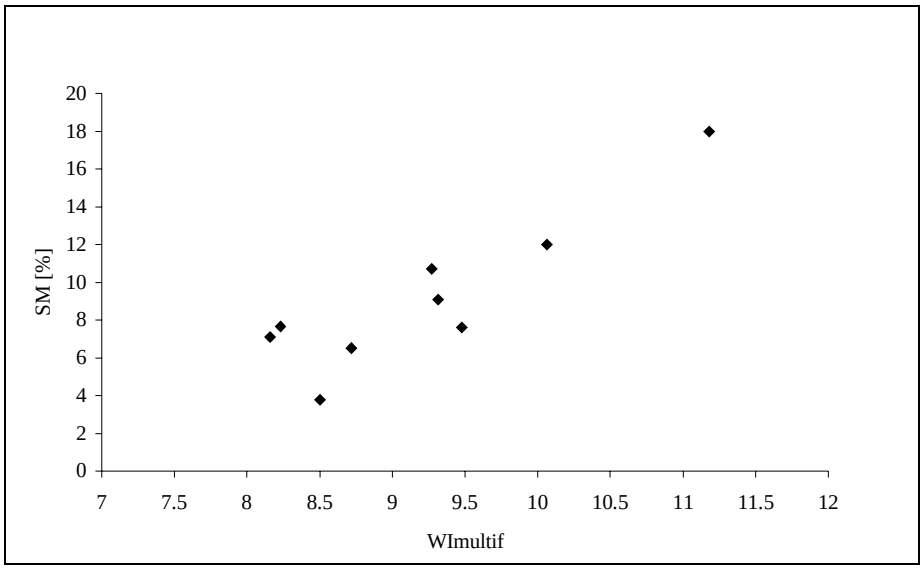

Figure 17. *Soil moisture plotted against the filtered wetness index based on multi-directional flow, WImultif, for the E transect.*

5.2.5 Transect F

The topography of the F transect ranges from 179 to 199 meters, along a homogeneous slope profile stretching from the north to the south (appendix 4). The slope of the individual sample points ranges from 0.04 to 2.66° with an average value of 1.17°. The soil moisture content varies between 4 and 23 percent with an average value of approximately 10 percent. According to the STI, "4" is the dominating texture class in the area, where there are more or less equal entities of agriculture and pasture.

Table 8 summarizes the result from a stepwise regression analysis and Durbin-Watson statistic for the F transect, using STI and VegCov as predictors. The best subset of predictors constitutes the model where only STI is included, which explains 68.9 percent of the variability in soil moisture. The F-value of the VegCov variable is not significant, why it was not incorporated in the model. Figure 18 shows STI plotted against SM. The residual plot of the regression equation shows that the residuals are fairly normally distributed, while the Durbin-Watson statistic fails to reject the hypothesis of autocorrelated residuals.

Table 8. *Regression equation and statistical measures for the F transect.*

Regression Equation	R^2	T-value	D
SM=-0.0370+0.0245STI	68.9	5.36	1.61

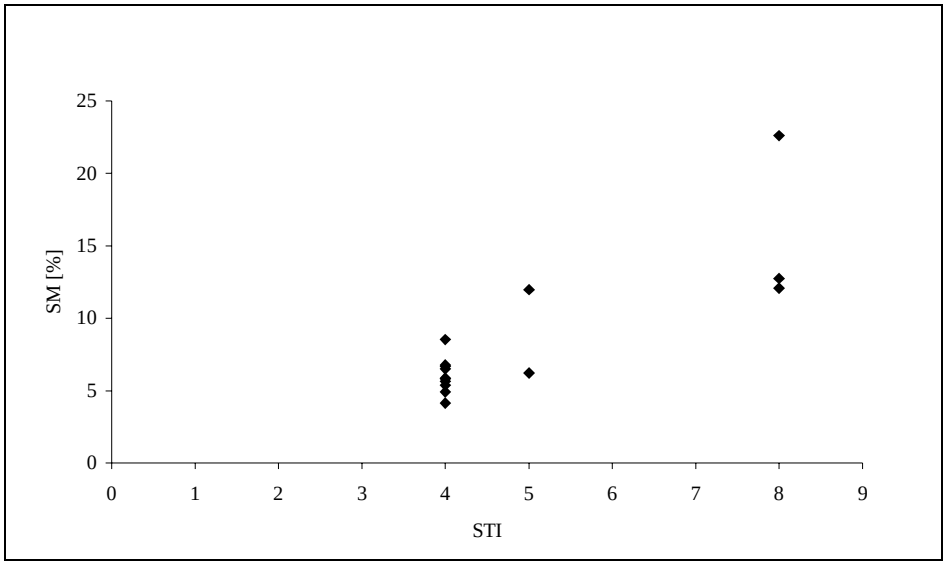

Figure 18. *Soil moisture plotted against the Soil Texture Index, STI, for the F transect.*

5.2.6 Transect G

The topography of the G transect (15 samples) ranges from 176 to 192 meters, along a uniform gentle slope in a north-southerly direction (appendix 4). The slope of the sample points varies between 0.34 and 0.86° with an average value of 0.52°. According to the STI, "4"is the dominating texture class in the area, where agriculture dominates the land use. The soil moisture content ranges from 4 to 15 percent with an average value of 7 percent.

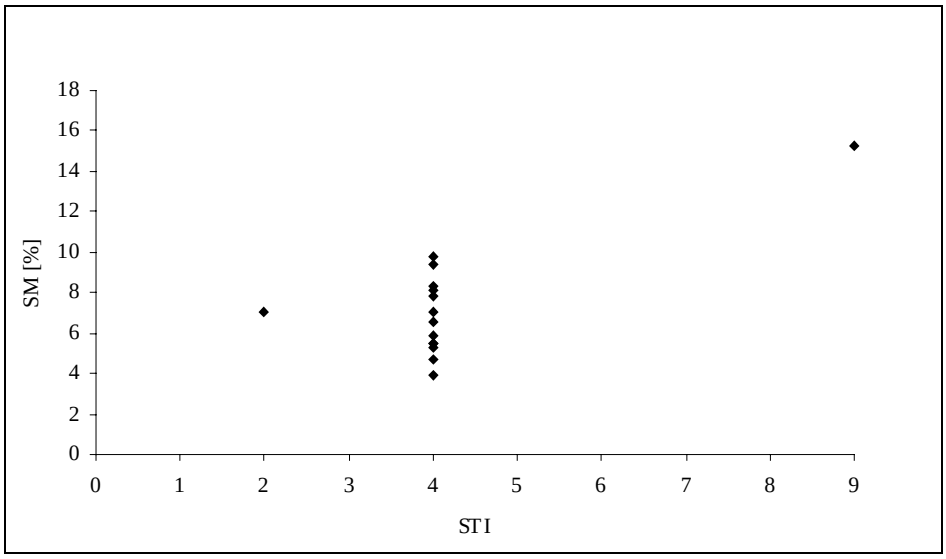

Figure 19. *Soil moisture plotted against the Soil Texture Index, STI, for the G transect.*

Table 9. *Regression equations and statistical measures for the G transect.*

Regression Equation	R^2	T-value MultiAf	T-value STI	D
SM=-0.0020+0.00402MultiAf+0.0106STI	79.3	3.93	3.90	1.79

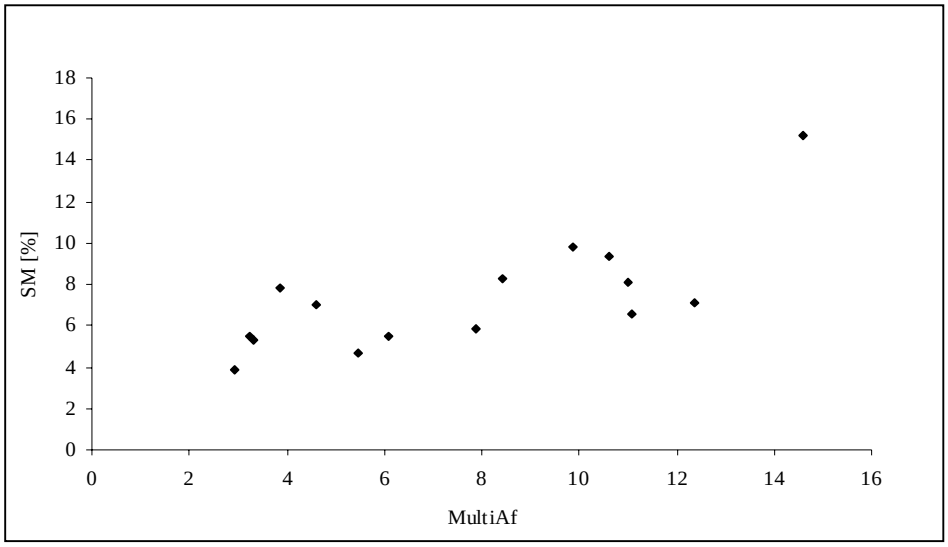

Figure 20. *Soil moisture plotted against filtered specific catchment area based on multi-directional flow, MultiAf, for the G transect.*

Table 9 summarizes the result from a stepwise regression analysis and Durbin-Watson statistic for the G transect, using STI, MultiA, MultiA/c, WImulti, MultiAf, MultiAf/c and WImultif. The best subset of predictors constitutes the model where MultiAf and STI are used in multiple regression. This model explains 79.3 percent of the distribution in soil moisture. Figure 19 shows STI plotted against SM, whereas figure 20 shows MultiAf plotted against SM. The Durbin-Watson statistic for the multiple regression equation shows that the hypothesis of autocorrelation in regression residuals can be rejected. According to the residual plot of the regression equation, the regression residuals are not normally distributed.

5.2.7 Transect H

The topography of the H transect (12 samples) ranges from 198 to 233 meters, along a stretch of undulating terrain in a north-east south-westerly direction (appendix 4). The slope of the individual sample points varies between 0.20 and 1.53° with an average value of 0.79°. According to the STI no specific texture class is overrepresented within the area where agriculture is the most common land use. The soil moisture content ranges from 4 to 24 percent with an average value of 12 percent.

Table 10 summarizes the result from stepwise regression analysis and Durbin-Watson statistic for the H transect, using STI and VegCov as predictors. The best subset of predictors constitutes the simple regression model including STI, which explains 83.9 percent of the variability in soil moisture. The F-value of the VegCov variable is not significant, why it was not incorporated in the model. Figure 21 shows STI plotted against SM. The regression residuals, however, shows that the residuals are far from

being normally distributed. A Durbin-Watson statistic is not available for this transect, since the number of samples is too low.

Table 10. *Regression equation and statistical measures for the H transect.*

Regression Equation	R^2	T-value
SM=-0.0429+0.0272STI	83.9	7.23

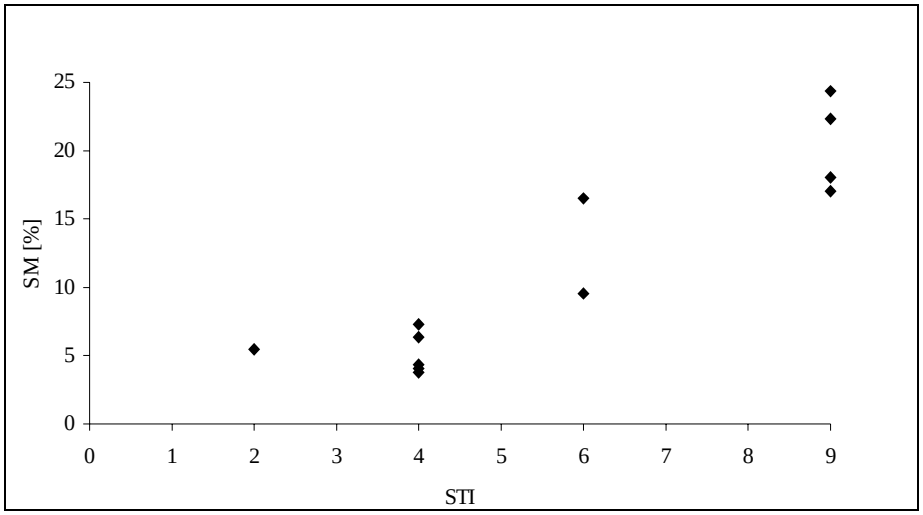

Figure 21. *Soil moisture plotted against the Soil Texture Index, STI, for the H transect.*

5.2.8 All Data

Table 11 summarizes the statistics for a regression involving STI and SM, using the complete data material. Figure 22 shows STI plotted against SM. By studying residual plots for the regression equation, it can be concluded that the residuals are normally distributed. The Durbin-Watson statistic points towards autocorrelation in the regression residuals. The F-value is higher than its corresponding critical value, which makes the regression equation suitable for predictions of soil moisture (table 12).

Table 11. *Regression equation and statistical measures for the complete data material.*

Regression Equation	R^2	D
SM=0.00557+0.0168STI	55.4	1.58

Table 12. *F-test statistics for the regression equation.*

F-value	Regression DF	Residual DF	Regression SS	Residual SS	Critical F-value
114.41	1	92	0.089108	0.071652	≈4

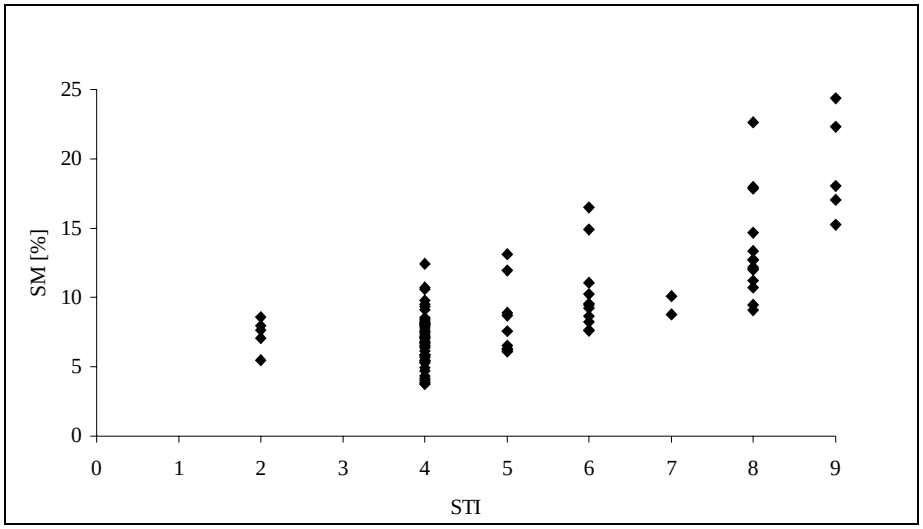

Figure 22. *Soil moisture plotted against the Soil Texture Index, STI, for the complete data material.*

5.2.9 Summary of Results

Table 13 summarizes topographic, vegetation and soil characteristics for the individual transects. The wetness index and specific cacthment area (filtered or unfiltered) is correlated with soil moisture in the case of the A, C, E and G transects, whereas in the B, F and H transects the relationship is insignificant. The highest correlation, 0.893, is found between the samples of the E transect and WImultif. The Soil Texture Index is correlated with soil moisture in all the individual transects as well as in the case of the complete data material. The highest correlation, 0.916, is found between the samples of the H transect and STI.

Table 13. *Vegetation, topographic and soil characteristics for the individual transects.*

Transect	Vegetation characteristics	Topographic characteristics	Dominating soil texture
A	Agriculture (Pasture)	• 200 to 246 meters, average 226 meters • uniform slope profile • average slope 0.56°	NO
B	Agriculture (Pasture)	• 194 to 260 meters, average 228 meters • undulating terrain • average slope 0.75°	NO
C	Pasture (Agriculture)	• 175 to 227 meters, average 206 meters • uniform slope profile • average slope 0.44°	STI 4
E	Agriculture (forest)	• 210 to 245 meters, average 229 meters • undulating terrain • average slope 1.04°	NO
F	Agriculture Pasture	• 179 to 199 meters, average 192 meters • uniform slope • average slope 1.17°	STI 4
G	Agriculture (Pasture)	• 176 to 192 meters, average 183 meters • uniform slope profile • average slope 0.52°	STI 4
H	Agriculture (Pasture)	• 198 to 233 meters, average 217 meters • undulating terrain • average slope 0.79°	NO

The stepwise regression analysis shows that in general, it is not advisable to incorporate the wetness index or the specific catchment area (filtered or unfiltered) in a regression model, except for in the case of the G and E transects. In the case of the

G transect, STI and MultiAf are combined to produce a multiple regression equation, explaining 79 percent of the spatial distribution in soil moisture. However, the regression equation is questionable, since the relationship between STI and soil moisture is rather doubtful (figure 19). In the case of the E transect WImultif is used in simple regression to produce a model, explaining 80 percent of the spatial distribution in soil moisture. In the remaining cases, the F-ratios of the topographic variables are too low to be allowed in the regressions.

According to the stepwise regression analysis, the use of STI in a regression model is justified in the case of the A, B, C, F, G and H transects. In the E transect, the F-value of STI is insignificant, why it is not used. The use of the Soil Texture Index in simple regression, incorporating the complete data material, results in a model that accounts for 55 percent of the spatial variation in soil moisture. This is the only derived equation that is applicable on the entire drainage basin.

5.3 Accuracy of the Digital Elevation Model

The evaluation in the field resulted in two graphical profiles showing the elevation information in the DEM compared to the measured values in the field (figures 23 & 24). The profiles show that the elevation extremes are not captured in the DEM, since valley bottoms and hilltops are somewhat underestimated in the interpolation procedure. It is also evident that the interpolation yields correct values at the locations of contours, whereas the interpolated values between the contours varies as a smoothing spline (figure 23).

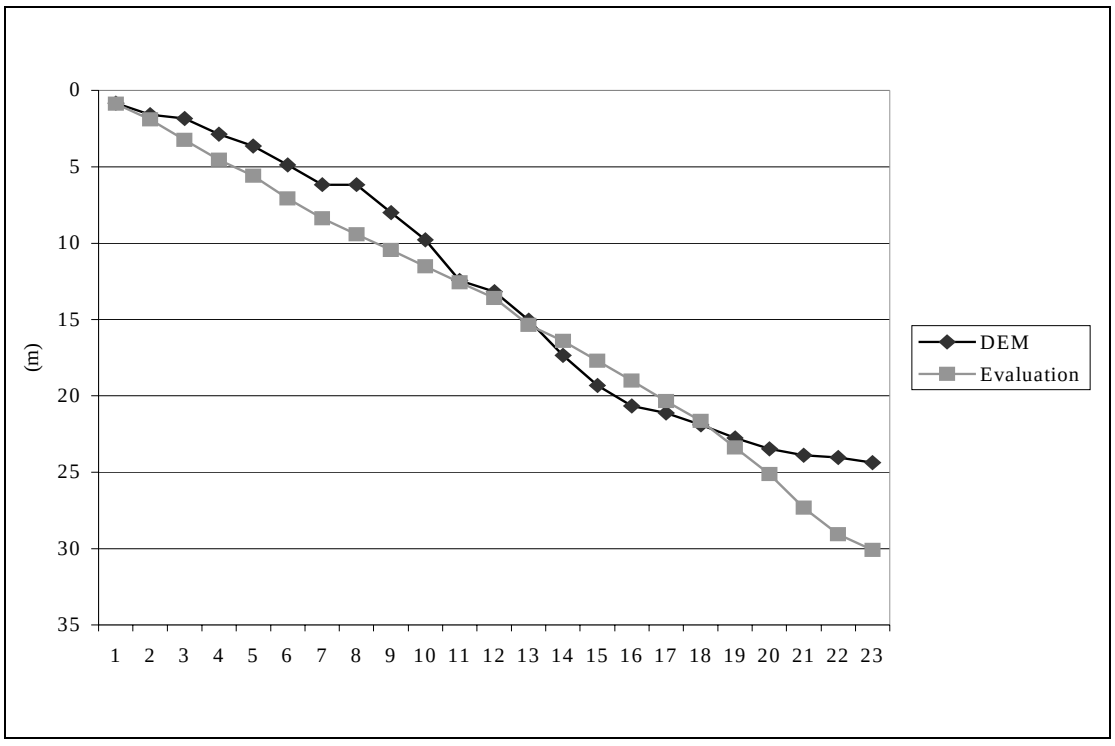

Figure 23. *Slope profiles nearby the SARI Manga agricultural station as defined by the DEM and by manual measurements. The X-axis shows an index number for each measurement point while the Y-axis describes relative height difference in meters.*

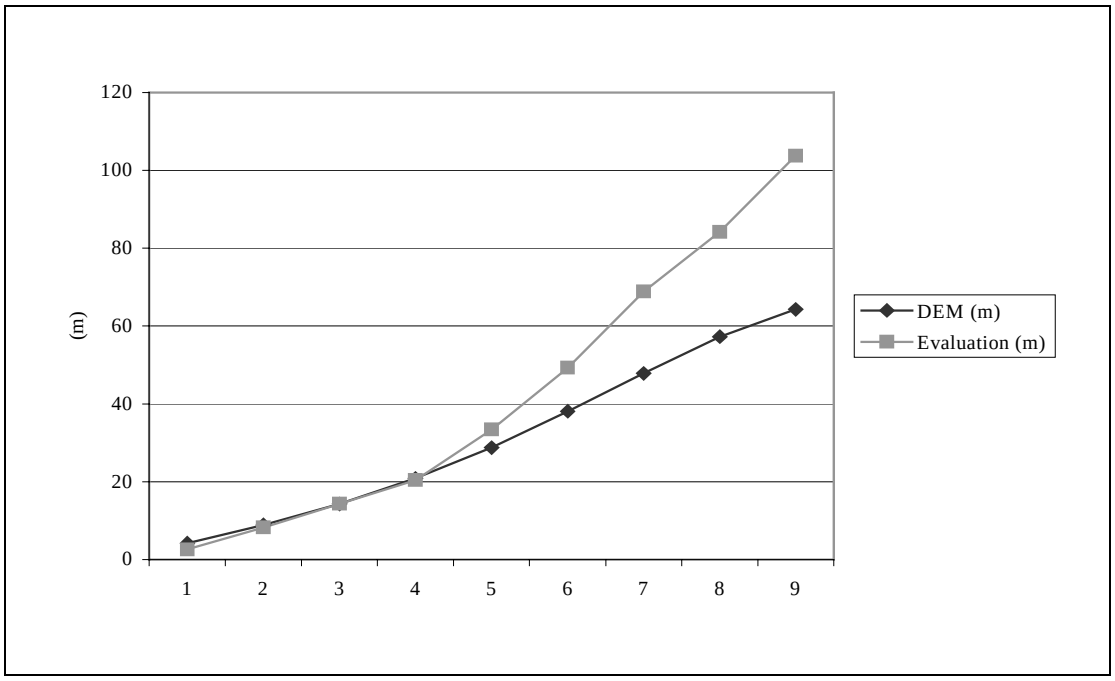

Figure 24. *Slope profiles at the single hill formation of the catchment, as defined by the DEM and by manual measurements. The X-axis shows an index number for each measurement point while the Y-axis describes relative height difference in meters.*

6 DISCUSSION

6.1 Topography

6.1.1 Issues Concerning the Construction of the DEM

Topographic features such as ridges, watersheds and drainage channels are important when conducting hydrological studies. Low resolution sampling data will result in a less detailed depicting of a terrain, unless streamline data and drainage enforcement algorithms, such as Hutchinson's ANUDEM, could be used. When the highest possible accuracy is needed, advanced algorithms like this offer more flexibility and higher precision (Eklundh & Mårtensson, 1995). It is also being routinely used by researchers in hydrologic modeling of small catchments (Moore et al., 1988).

When interpolating a DEM, the best result is usually achieved when the data points are well distributed throughout the interpolation area. Contour lines are practical when illustrating a landscape, but they do not represent the surface in a statistically correct way since points along the lines are over-represented compared with the ones perpendicular to them (Eklundh, 1999). Problems related to the interpolation, such as internal drainage and obscure sinks, appeared during the construction of the DEM where information on the terrain was inadequate.

Programs that account for the extents of basins and drainage networks should be used on materials that contain spurious sinks (Marks et al., 1984), and by applying the Arc/Info Drainage Enforcement Algorithm inherent in the Topogrid module, the problems with the internal drainage disappeared. The Filldem operation in Arc/Info processed the DEM effectively, and in a later search for sinks using the ArcView hydrological extension, no sinks were found. Having made these adjustments, the DEM seemed to be hydrologically sound. Without the use of the drainage algorithm and the incorporation of the streamline data, the DEM would not be reliable and hence not suitable for extractions of wetness indices.

The sink issue is controversial, since sinks are natural features in some landscapes, whereas they are a product of the interpolation procedure in others. Natural features should be preserved in order to maintain a true representation of reality. The removal of sinks in this study is based on the knowledge that the low-relief terrain of the Tamne River Basin does not contain such features. The sinks that previously occurred in the DEM were most likely a result of the interpolation process, since the input data was too sparsely distributed to depict such small-scale topographic entities.

As shown in figures 23 and 24, the DEM shows values less extreme than those of the field measurements. When the measurement values increase or decrease as the profiles approach their local maximum and minimum respectively, the DEM values tend to flatten out. The local maxima and minima do occur at the proper locations, but the values are either too high in the valleys, or too low on the hilltops. The reason for this might be the low resolution, an equidistance of 15 meters, in the elevation contour data that was available for the interpolation of the DEM. Additional elevation data values could have been used gathered from valley bottoms and other topographic

features, but these samples would have been estimations by manual methods since the GPS receiver showed very incorrect elevation values.

Due to the low relief of the landscape, the long distances between the isolines give uncertainties in the interpolated material. To this should be added the fact that the topographic contour information is almost 40 years old, why denudation through erosion since then most likely has occurred.

The impact of the exaggerated smoothing at elevation extremes on derived wetness index values might be a less concentrated flow of water, thus creating more widespread water channels. The flattened valley bottoms will also result in an overestimation of wetness index values since the slope angle is lower than that of the true terrain. These assumptions, however, are most likely not pertinent in this study since few samples were collected from the soil of the valley bottom. Furthermore, the chosen resolution of the DEM would not permit a much-improved representation of these small-scale features.

It is worth mentioning that the method of measuring the slope angle in a clinometer over a distance of 50 meters is possible, but not very precise. The accuracy of the measurements is estimated at a height difference of around 0.2 meters (based on the estimated accuracy of the clinometer at 1/4°), which means that the SARI profile, in particular, could have shown a better resemblance with the interpolated material.

6.1.2 Studies Concerning Wetness Indices

Moore et al. (1988) concluded that the wetness index accounted for 26 to 33 percent of the variability in soil moisture when investigating a 7.5 hectare drainage basin in New South Wales, Australia. The best estimate was achieved using the wetness index and aspect in multiple regression (31 to 41 percent). In a 38 hectare catchment in Kansas, Ladson & Moore (1992) found that the wetness index explained less than 10 percent of the soil moisture distribution. Nyberg (1996) concluded that the wetness index explained 34 percent of the spatial distribution in soil moisture when studying a 0.63 hectare Swedish catchment. In a 12.5 km^2 catchment on the Swiss Plateau, Jordan (1994) found that the wetness index explained 3 to 79 percent of the spatial distribution in soil moisture on seven occasions. Less than 25 percent of the variance was explained on five of the seven occasions. Western et al. (1999) showed that for a 10.5 hectare catchment in Tarrawarra, Australia, combinations of $\ln(a)$ or $\ln(a/\tan\beta)$ and a potential solar radiation index, explained up to 61 percent of the spatial distribution in soil moisture during wet periods and up to 22 percent during dry periods.

The predictive power of the topographic wetness index has so far not showed a consistent result. The explained variance varies greatly between studies and within studies and is, in most cases, relatively low. Coefficients of determination in this study are of the same magnitude as the results from the studies presented above, ranging from unreasonably low values (zero correlation) to 80 percent. The important questions to address are:

- The reason why the wetness index seems to work on some transects and not on others

- How the conditions that prevailed in the catchment during the field work may have influenced the result
- If the use of the wetness index is justified in the Tamne River Basin, considering the assumptions inherent in the method

6.1.3 Sampling Strategy & Input Data

The studies of vegetation and soil characteristics for each transect reveal no specific difference between transects, where the wetness index is or is not a suitable predictor. Nor do the topographic characteristics of the individual transects show substantial differences. However, the DEM may not constitute a true representation of reality in all parts of the terrain. Considering the relatively old topographic data from which the DEM was derived, both natural and anthropogenic influences during the years may have altered the landscape. Furthermore, the resolution of the DEM may not capture small-scale topographic features that are important for the distribution of soil moisture. The total effect of this may explain the poor performance of the wetness index in some parts of the study area.

Another factor that most likely has influenced the results is the chosen sampling strategy. A disadvantage of using point samples for hydrological studies is the points being notoriously poor in identifying spatial organization. The random appearance of hydrological variables often observed is, to some part, caused by this relationship (Western et al., 1999). A better result might have been achieved if additional soil samples had been taken at each sample site and if the average of these samples had then been used. Furthermore, the road sampling method is perhaps not ideal since the distribution of points is limited. The human impact on the areas in the vicinity of roads is greater than on the surroundings, which means that a bias component is introduced in the data material.

The drilling procedure can be criticized because of a few unsuccessful penetration attempts in coarse-grained soils, especially in the end of the sampling period, when the soil had been exposed to drought. The unsuccessful attempts have most likely resulted in less soil moisture and therefore have increased the unexplained variance within the data sets. Another bias component introduced at sample points with extremely dry soils, is collapsing walls of the drilled borehole. This may have caused some soil samples to be less representative in a context of samples taken at the 20 – 30 centimeter level.

Finally, the soil samples were collected over a period of two weeks, during which time the moisture content of the soil decreased continuously. This means that the data are somewhat biased when analyzing the complete data material.

6.1.4 The Predictive Ability of Wetness Indices

The critical question when investigating soil water distribution in an area through wetness indices, is if the method is capable of accurate predictions, considering the simplicity of the approach versus physical processes in a catchment. Moore and Hutchinson (1991, p.806) argued “only the spatial variability of topographic attributes and net rainfall need to be considered to provide adequate estimates of the spatial variability of soil water content. The other parameters can be lumped with little or no loss in predictive ability”. This statement is not necessarily true for all climates and topographic settings. In areas of low relief, topography may be secondary in relation

to other parameters, such as vegetation and soil properties. Furthermore there are other factors limiting the use of the wetness index. According to Western et al. (1999), a random and an organized component constitute the observed spatial distribution of soil moisture. This means that an upper limit exists that determines the maximum explained variance that can ever be achieved in an area. Another important issue is that the most commonly used wetness indices are independent of time, which means that the correspondence between soil moisture and wetness index varies throughout the year. Ladson (1990) found that the spatial variability in soil moisture was significant during the winter while no differentiation could be observed during the summer (all sites being equally dry).

As mentioned in the theory section, a number of more or less questionable assumptions underlie the use of topographic wetness indices in a drainage basin:

1. The water table is parallel to the soil surface
2. The saturated hydraulic conductivity decreases exponentially with depth
3. Steady state conditions prevail in the catchment
4. The groundwater recharge rate is uniform.

According to Seibert (1997), assumptions 1 and 2 are in general found to be reasonable, whereas number 3 and 4 constitute a greater conflict with reality.

The assumption of a spatially uniform recharge rate to the groundwater means that it is assumed that the amount of rainfall is equal in all parts of the catchment, evapotranspiration is spatially uniform and the hydraulic conductivity profile is uniform over the area. Considering the size of the Tamne River Basin (approximately 800 km^2), the heterogeneity in soil type and underlying bedrock, these conditions are most likely not met in reality. As Rodhe & Seibert (1999) stated, the inhomogeneous soil, varying soil thickness, varying underlying bedrock and occurrence of exposed bedrock must cause the conductivity profile to vary greatly. A consequence of this fact could be observed at a number of places in the study area, where small ponds of water were present at higher altitudes, dammed by an impermeable soil layer or exposed bedrock. These occurrences can never be captured by the wetness index in its present form.

By studying precipitation records for Garu and SARI meteorological stations, both situated within the Tamne River Basin at a distance of approximately 20 kilometers from each other, the spatial and temporal variations become clear. Figure 25 shows the September rainfall total from 1979 to 1990 for Garu and SARI meteorological stations. This information points towards the fact that the assumption of uniform precipitation is severely violated when considering the entire drainage basin.

The impact of a spatially uniform recharge rate on the expected relationship between soil moisture and the wetness index is probably substantial when examining the complete data material, but less important investigating the individual transects. When examining the relationship between soil moisture and the topographic wetness index for individual transects, the assumption of uniform precipitation and evapotranspiration is more or less justified. However, the soil properties are still expected to vary widely in the proximity of the transects, which may have a significant impact on the variability in soil moisture. The effect of a spatially uniform

recharge rate makes the study of individual transects in limited areas more interesting. It has most likely contributed to the low correlation between soil moisture and the wetness index when examining the complete data material. The extreme conditions that prevailed in the study area prior to the field study are worth mentioning, when unusual amounts of precipitation and the opening of dams in Burkina Faso caused flooding and generally high water levels in large parts of northern Ghana. The effect of this upon the heterogeneity of ground water recharge, through prolonged precipitation, is hard to determine.

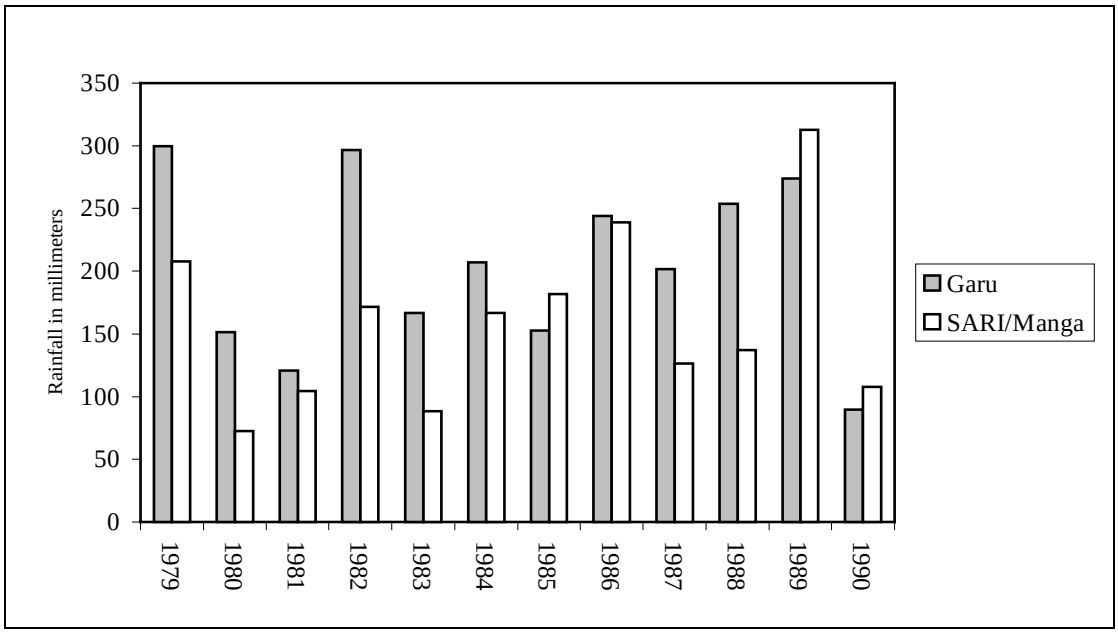

Figure 25. *Yearly rainfall totals for the years 1979 – 1990 at the SARI Manga and Garu Natinga meteorological stations.*

The steady state assumption in the topographic wetness index has been criticized for being invalid for a number of climates and topographic characteristics (Western et al., 1999). This is because the approach does not consider different topographic settings and soil properties within a local drainage basin, which could increase or decrease the specific catchment area. Considering two local drainage areas of equal size, having different topographic characteristics and soil properties, the steady state approach would produce two specific drainage areas of equal size. This is most likely not the case in reality, since spatial variations in soil properties (drainage capacity) control the time required for water to reach the outlet of a local drainage area, and thereby the size of the specific catchment area. Furthermore, the topographic characteristics of a local drainage area govern the hydraulic gradient, which determines the drainage velocity, and the proximity of the local drainage area to its outlet.

Taking into consideration the gentle and relatively uniform slopes of the Tamne River Basin, the effect of slope gradient on spatial differences in drainage velocity is considered small in relation to the impact of changing soil properties. The proximity of a local drainage area to its outlet is crucial, however, since the drainage velocities of the catchments are small, due to the low slope gradients. The outlets of two local drainage areas of equal size, one having the bulk of its area close to its outlet and the other having a more remote area, are probably not influenced by two identical specific

drainage areas. The moderate topography of the study area results in very low drainage velocities, causing parts of remotely situated local drainage areas to be excluded from the specific drainage area, while local drainage areas located in the proximity of an outlet are favored.

According to Barling (1994), the elevation potential dominates the subsurface water movement on steep slopes (>6°), while the soil water matrix becomes more important in areas of low relief (<6°). As mentioned before, this constitutes a major drawback of the steady state wetness index. Barling (1994) further showed that the value of the dynamic wetness index approaches the corresponding value of the static index as the drainage time increases. It is, however, unlikely that it will reach steady state unless the drainage time is unrealistically high. The correlation between simulated water table depths (calculated in a dynamic rainfall – runoff model called Thales) and the dynamic wetness index was considerably higher compared with the correlation when the static wetness index was used (R^2 of 0.8 for the dynamic index compared with 0.3 for the static one). However, according to Siebert (1997), there are serious drawbacks in the derivation of the "quasi-dynamic" wetness index by Barling (1994). The assumption of a spatially uniform recharge rate is still present and, moreover, it is constant during the specified drainage time (Siebert, 1999).

The effort in this study, to relax the steady state assumption, did not, however, improve the predictive power of the wetness index. This is most likely not due to extensive errors in the theory behind the non steady state wetness index, but rather the result of the simplified implementation used. First of all, the implementation used in this study defines the time dependent specific drainage area in terms of entire pixels. Due to the relatively coarse resolution of the DEM some of the rationale of the approach is lost because of this. Secondly, due to lack of suitable soil data regarding hydraulic conductivity, the impact of varying soil properties was not captured. The individual drainage time of each pixel was calculated from its local slope, resulting in a "time index" rather than drainage time, since data on hydraulic conductivity and effective porosity was not known.

A number of previous studies have pointed out that soil moisture distribution is depending on different parameters as the season changes. Famiglietti et al. (1998) found that the influencing parameters changed from control by soil heterogeneity, following an intense rainfall event, towards joint control by topography and soil properties when the soil dried (along a hillslope transect at Rattlesnake Hill, Texas). During dry conditions, the soil moisture was better correlated with other topographic attributes than the wetness index, such as relative elevation and aspect (Famiglietti et al., 1998). According to a study by Western et al. (1999), the wetness index explained up to 61 percent of the spatial variation in soil moisture during wet conditions and up to 22 percent during dry periods. This study further recognizes the need for wetness indices that account for the changes in dominant processes taking place during the year (Western et al., 1999).

The fact that the predictive ability of the wetness index decreases under dry conditions is not surprising. The wetness index was not developed for predictions of moisture content in the upper part of the soil profile, but for estimations of relative depth to the water table (Famiglietti et al., 1998). As mentioned before, the depth to the water table has a large impact on the soil water content. As the depth to the water

table increases, the soil water content decreases and vice versa. However, this is only true for relatively shallow ground water levels. If the depth to the water table is sufficient, no equilibrium between the ground water table and soil water will arise. The equilibrium constitutes the state where the depth to the ground water table influences the soil water content (Grip & Rodhe, 1994). During the relatively prolonged dry periods often experienced in the study area, the water table depths are most likely not shallow. This means that the wetness index is not suitable for predictions of soil moisture during these times of the year.

Considering this fact, it is important to make clear that our results are limited in time and to some part influenced by the unusual conditions prevailing in the catchment prior to our fieldwork, i.e. ground water levels that are not representative of normal conditions. The applicability of wetness indices in the Tamne River Basin is most likely subject to variations in efficiency, depending on the season. Considering the results of other studies, the time of fieldwork may coincide with a period when the influence of topography peaks. The results might therefore only be valid for predictions of soil moisture during this period of time, i.e. the wet season.

6.2 Soil & Vegetation

Reynolds (1970a, b) showed that variations in soil moisture could be related to soil texture, whereas Hawley et al. (1983) found that differences in soil moisture due to differences in soil texture were more apparent in wet conditions than in dry. Niemann & Edgell (1993) found that macroporosity wields influence on the moisture movement and hence the soil moisture variability. These conclusions are supported by the results of this study, where the Soil Texture Index is a suitable predictor for the individual transects as well as for the complete data material. The results might have been even better if the texture index had been based on a more thorough method, e.g. sifting and sedimentation analysis. The soil texture seems to be the dominant parameter for the distribution of soil moisture under moist conditions in the Tamne River Basin. We do not know much about its importance under dry conditions, but its relevance is probably less significant. The use of derived statistical models including STI for computations of soil moisture distribution are limited however, since required input soil data is insufficient. The available digital soil data map is very generalized and greater variations can be expected in the drainage basin.

Reynolds (1970b, c) noted that the vegetation density was one of the more important factors affecting soil moisture variability, and that the variability increased with a decreasing canopy cover. Francis et al. (1986) could see considerable differences in moisture content in areas of different vegetation cover and Hawley et al. (1983) noted that these differences were greater on wetter than on dry days.

The effect of a varying vegetation cover on the distribution in soil moisture was not captured by the simple method used in this study. On the other hand, given the relatively large-scale survey of this study, the vegetation cover may not account for a large part of the spatial distribution in soil moisture. From a larger perspective, the vegetation cover of the Tamne River Basin is relatively uniform (figure 26). The important aspect of this may not be whether the vegetation index is correlated with soil moisture or not, but rather if the vegetation cover tends to influence the effect of

topography. According to Hawley et al. (1983), the presence of a vegetation cover has a tendency to reduce the variations explained by topography. However, by studying the vegetation characteristics of transects where the wetness index performed well and where it did not, reveal that no significant differences in vegetation cover exist between the two groups. Having said that, does not mean that the vegetation is unimportant, but it is unlikely that it causes significant changes in spatial soil moisture distribution in this area and at the scale chosen for his study.

Figure 26. *Overview of the southern part of the Tamne River Basin, showing the moderate topography and evenly distributed vegetation. The photograph was taken from the Birrimian hill formation, being the only topographic deviation in the catchment.*

6.3 Combinations of Topographic Attributes & Soil Properties

The attempts made to combine topographic attributes and soil properties in a statistical model, in order to increase the explained variance, were not successful. In general (except for the E and G transects), predictors related to topography had non-significant F-values, which made them inappropriate for incorporation in regression models. However, even if the F-ratios of the topographic variables had been significant, multiple regression models including soil texture and wetness indices may not account for a larger part of the spatial distribution in soil moisture, compared to one-predictor models. This may be due to the intercorrelation observed between the Soil Texture Index and wetness index on some of the transects. The intercorrelation means that the predictors explain almost the same variance in soil moisture. The relationship between the wetness index and Soil Texture Index, however, is not surprising. According to Moore & Hutchinson (1991), pedogenesis is linked to the way water moves through the landscape. Because of this, topographic attributes that describe these flow paths inherently capture the spatial variation in soil properties.

7 CONCLUSIONS

The DEM corresponds well to the landscape morphology, except on hilltops and in valley bottoms. The latter is due to the sparsely distributed topographic input contours that are also out of date. The hydrological conditioning of the DEM, by application of a drainage enforcement algorithm together with streamlines, has shown to be necessary when conducting topographic modeling of hydrological processes.

This study shows that the use of wetness indices based on one-directional flow constitutes a far too simplified representation of reality. The derivation of flow networks using multi-directional flow algorithms is far more preferable within this context. The methods offered in commercial GIS packages are therefore not suitable for derivations of topographic wetness indices in areas like the Tamne River Basin.

Due to the heterogeneity in soil properties and precipitation in the Tamne River Basin, the applicability of the topographic wetness index is limited when considering the entire drainage basin. However, the use of the index in small homogeneous sub-drainage basins is probably justified under wet conditions. The link between soil water content and the ground water table is significant during times of shallow water table depths, which means that the use of the index is restricted in time as well. Other topographic attributes than the topographic wetness index may be useful in estimating the spatial distribution in soil moisture during dry periods.

The soil texture seems to constitute the most important variable (among those under consideration in this study) for distribution of soil moisture, under wet conditions, in the Tamne River Basin. The statistical model including soil texture is applicable on the entire drainage basin, but since high-resolution data concerning soil properties is not available, its use is limited.

REFERENCES

Allotey, J.A., Boateng, E., Duadze, S.E.K., 1998, Country report – State of land, water and plant nutrition in Ghana, *Regional Workshop on Land Vulnerability Assessment for Food Security using AEZ/LRIS Information*, Cotonou, Benin.

Barling, R.D., Moore, I.D. & Grayson, R.B., 1994, A quasi-dynamic wetness index for characterizing the spatial distribution of zones of surface saturation and soil water content, *Water Resources Research*, **30:4**.

Beven, K.J., & Kirkby, M.J., 1979, A physically based, variable contributing area model of basin hydrology, *Hydrological Sciences Bulletin*, **24:1**.

Cunin, N., 1993, Water balance and crop production – a case study from Northern Ghana. In: C. Seifert (ed.), 1997, Fieldstudies from Ghana – A presentation of surveys carried out by Danish students, *Geographica Hafniensia*, **C5**, Institute of Geography, University of Copenhagen, Denmark.

P.A. Burrough & R.A. McDonnell, (eds.), 1998, Principles of geographical information systems, *Spatial information systems and geostatistics*, Oxford University Press, Oxford.

Department of Quaternary Research, 1995, Kompendium i jordartsanalys – laboratorieanvisningar, *Quaternaria Ser. B: Rapporter & meddelanden*, **1**, Stockholms Universitet.

Dickson, K.B. & Benneh, G., 1988, A new geography of Ghana, Longman, Harlow.

Dingman, S.L., 1993, Physical Hydrology, Prentice-Hall Inc., Englewood Cliffs, New Jersey.

Eklundh, L., 1999, Interpolation av rumsliga data. In: L. Eklundh, (ed.): Geografisk informationsbehandling – metoder och tillämpningar, Byggforskningsrådet, Stockholm.

Eklundh, L. & Mårtensson, U., 1995, Rapid generation of Digital Elevation Models from topographic maps, *International Journal of Geographical Information Systems*, **9:3**.

ESRI, 1997, Arc/Info Help, version 7.2.1.

FAO, 1967, Land and Water Survey in the Upper and Northern Regions, Ghana, Final Report, *Soil Surveys*, **vol. 3**, Rome.

Famiglietti, J.S., Rodell, M, Rudnicki, J.W., 1998, Variability in surface content along a hillslope transect: Rattlesnake Hill, Texas, *Journal of Hydrology*, **210**.

Fitzpatrick, E.A., 1986, An introduction to soil science, Longman Scientific & Technical, Harlow, England.

Francis, C.F., Thornes, J.B., Romero Diaz, A., Lopez Bermudez, F. & Fisher, G.C., 1986, Topographic control of soil moisture, vegetation cover and land degradation in a moisture stressed Mediterranean environment, *Catena*, **13**. In: Famiglietti, J.S., Rodell, M, Rudnicki, J.W., 1998, Variability in surface content along a hillslope transect: Rattlesnake Hill, Texas, *Journal of Hydrology*, **210**.

Freeman, G.T., 1991, Calculating catchment area with divergent flow based on a regular grid, *Computers and Geosciences*, **17**. In: P.A. Burrough & R.A. McDonnell, (eds.), 1998, Principles of geographical information systems, *Spatial information systems and geostatistics*, Oxford University Press, Oxford.

Golub, G.H. & Van Loan, C.F., 1983, Matrix Computations, John Hopkins University, Baltimore. In: Hutchinson, M.F., 1989, A new procedure for gridding elevation and stream line data with automatic removal of spurious pits, *Journal of Hydrology*, **106**.

Grip, H. & Rodhe, A., 1994, Vattnets väg från regn till bäck, Hallgren & Fallgren Studieförlag AB, Uppsala.
Holmertz, G., 1996, Ghana Burkina Faso, L. Karlsson, (ed.), *Länder i fickformat*, **305**, The Swedish Institute of International Affairs, Stockholm.
Hawley, M.E., Jackson, T.J., McCuen, R.H., 1983, Surface soil moisture variation on small agricultural watersheds, *Journal of Hydrology*, **62**.
Hornberger, G.M., Raffensperger, J.P., Wiberg, P.L. & Eshleman, K.N., 1998, Elements of Physical Hydrology, The John Hopkins University Press, Baltimore.
Hutchinson, M.F., 1988, Calculation of hydrologically sound digital elevation models, *Proceedings of the Third International Symposium on Spatial Data Handling*, August 17-19, Sydney. International Geographical Union, Columbus, Ohio.
Hutchinson, M.F., 1989, A new procedure for gridding elevation and stream line data with automatic removal of spurious pits, *Journal of Hydrology*, **106**.
Hutchinson, M.F., 1991, ANUDEM Manual, Centre for Resource and Environmental Studies, Australian National University.
Iida, T., 1984, A hydrological method of estimation of topographic effect on saturated throughflow, *Trans. Jap. Geomorphol. Union*, **5:1**. In: Barling, R.D., Moore, I.D. & Grayson, R.B., 1994, A quasi-dynamic wetness index for characterizing the spatial distribution of zones of surface saturation and soil water content, *Water Resources Research*, **30:4**.
Instituto del Tercer Mundo (ed.), 1999, The world guide 1997/1998: a view from the south, New Internationalist Publications, Oxford.
Jordan, J.P., Spatial and temporal variability of stormflow generation processes on a Swiss catchment, *Journal of Hydrology*, **152**.
Ladson, A.R., 1990, Soil water predictions by microwave remote sensing and topographic attributes, Unpublished M.S. thesis, University of Minnesota, St Paul. In: Barling, R.D., Moore, I.D. & Grayson, R.B., 1994, A quasi-dynamic wetness index for characterizing the spatial distribution of zones of surface saturation and soil water content, *Water Resources Research*, **30:4**.
Ladson, A.R. & Moore, I.D., 1992, Soil water predictions on the Konza Prairie by microwave remote sensing and topographic attributes, *Journal of Hydrology*, **138:3-4**.
Madsen, C. & Hulmose Nielsen, F., 1991, Compound farming in north-east Ghana. In: C. Seifert (ed.), 1997, Fieldstudies from Ghana – A presentation of surveys carried out by Danish students, *Geographica Hafniensia*, **C5**, Institute of Geography, University of Copenhagen, Denmark.
Mark, D.M., 1984, Automated detection of drainage networks from Digital Elevation Models, *Cartographica*, **21**.
Marks, D., Dozier, J. & Frew, J., 1984, Automated basin delineation from digital elevation data, *Geo-proc*., **2**. In: Hutchinson, M.F., 1989, A new procedure for gridding elevation and stream line data with automatic removal of spurious pits, *Journal of Hydrology*, **106**.
Minitab Inc., 1998, Minitab Help, release 12.1.
Moore, I.D., Burch, G.J. & Mackenzie, D.H., 1988, Topographic effects on the distribution of surface water and the location of ephemeral gullies, *Trans. Am. Soc. Agric. Eng.*, **31**. In: Famiglietti, J.S., Rodell, M, Rudnicki, J.W., 1998, Variability in surface content along a hillslope transect: Rattlesnake Hill, Texas, *Journal of Hydrology*, **210**.
Moore, I.D., 1996, GIS and Environmental Modelling; Progress and Research Issues, GIS World Books, Fort Collins, Colorado. In: P.A. Burrough & R.A. McDonnell,

(eds.), 1998, Principles of geographical information systems, *Spatial information systems and geostatistics*, Oxford University Press, Oxford.

Moore, I.D. & Hutchinson, M.F., 1991, Spatial Extension of Hydrologic Process Modelling, *Proceedings of the International Hydrology and Water Resources Symposium*, p.806. In: Barling, R.D., Moore, I.D. & Grayson, R.B., 1994, A quasi-dynamic wetness index for characterizing the spatial distribution of zones of surface saturation and soil water content, *Water Resources Research*, **30:4**.

Niemann, K.O. & Edgell, M.C.R., 1993, Preliminary analysis of spatial and temporal distribution of soil moisture on a deforested slope, *Physical Geography*, **5:14**.

Nyberg, L., 1996, Spatial variability of soil water content in the covered catchment at Gårdsjön, Sweden, *Hydrological Processes*, **10**.

Pilesjö, P., Zhou, Q. & Harrie, L., 2000, Estimating Flow Distribution over Digital Elevation Models Using a Form-Based Algorithm, *Journal of Geographical Information Science* (in press).

Quinn, P., Beven, K., Chevalier, P. & Planchon, O., 1991, The prediction of hillslope flow paths for distributed hydrological modeling using digital terrain models, *Hydrological Processes*, **5**.

Reynolds, S.G., 1970, The gravimetric method of soil moisture determination, I: A study of equipment, and methodological problems, *Journal of Hydrology*, **11**.

Reynolds, S.G., 1970, The gravimetric method of soil moisture determination, II: Typical required sample sizes and methods of reducing variability, *Journal of Hydrology*, **11**.

Reynolds, S.G., 1970, The gravimetric method of soil moisture determination, III: An examination of factors influencing soil moisture variability, *Journal of Hydrology*, **11**.

Rodhe, A., Seibert, J., Wetland occurance in relation to topography – a test of topographic indices as moisture indicators, *Agricultural & Forest Meteorology*, **98-99**.

Seibert, J., 1997, On Topmodel's ability to simulate ground water dynamics, *Regionalization in Hydrology*, **254**, IAHS Publication.

Shaw, G. & Wheeler, D., 1996, Statistical Techniques in Geographical Analysis, David Fulton Publishers, London.

C. Seifert (ed.), 1997, Fieldstudies from Ghana – A presentation of surveys carried out by Danish students, *Geographica Hafniensia*, **C5**, Institute of Geography, University of Copenhagen, Denmark.

Sivapalan, M., Beven, K. & Wood, E. F., 1987, On hydrologic similarity 2. A scaled model of storm runoff production, *Water Resources Research*, **23**.

Western, A.W., Grayson, R.B., Blöschl, G., Willgoose, G.R. & McMahon, T.A., 1999, Observed spatial organization of soil moisture and its relation to terrain indices, *Water Resources Research*, **35:3**.

Young, D.M., 1971, Iterative solution of large linear systems, Academic Press, New York. In: Hutchinson, M.F., 1989, A new procedure for gridding elevation and stream line data with automatic removal of spurious pits, *Journal of Hydrology*, **106**.

Zaslavsky, D. & Rogowski, A.S., 1969, Hydrologic and morphologic implications of anisotropy and infiltration in soil profile development, *Soil Sci. Soc. Am. Proc.*, **33**. In: Barling, R.D., Moore, I.D. & Grayson, R.B., 1994, A quasi-dynamic wetness index for characterizing the spatial distribution of zones of surface saturation and soil water content, *Water Resources Research*, **30:4**.

INTERNET REFERENCES

1. http://lcweb2.loc.gov/frd/cs/cshome.html The Library of Congress "Country Studies" (USA), data as of November 1994.
2. http://www.fao.org/ag/AGL/AGLW/AQUASTAT/ghan.htm Food and Agriculture Organization of the United Nations, Aquastat, data as of October 1995.
3. http://www.fao.org/ag/agl/swlwpnr/GHANA/HOME.HTM Food and Agriculture Organization of the United Nations, Land and Water Development Division, country profile of Ghana.
4. http://www.fao.org/ag/aga/agap/frg/ Food and Agriculture Organization of the United Nations, Feed Resources Group.
5. http://cres.anu.edu.au/software/anudem.html Description of the ANUDEM software at the Centre for Resource and Environmental Studies, as of April 1998.

Appendix 1

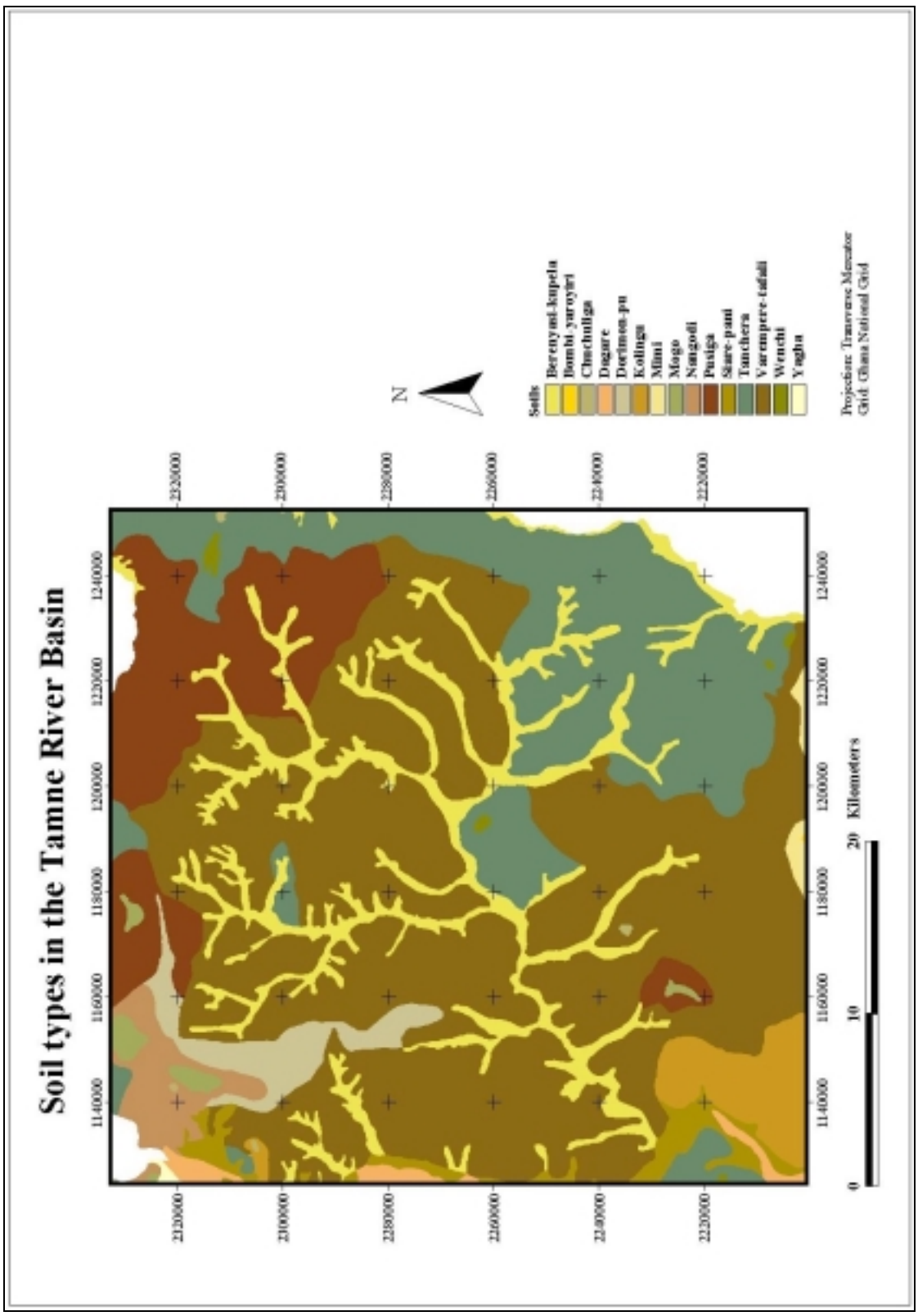
Soil types in the Tamne River Basin
N
Soils
Berenyasi-kupela
Bombi_yaroyiri
Chechuliga
Degure
Derlimen-pu
Kolinga
Mimi
Mogo
Nangodi
Pusiga
Sare-pani
Tanchera
Varempere-fadali
Wenchi
Yagha
Projection: Transverse Mercator
Grid: Ghana National Grid
0
10
20
Kilometers

Appendix 2

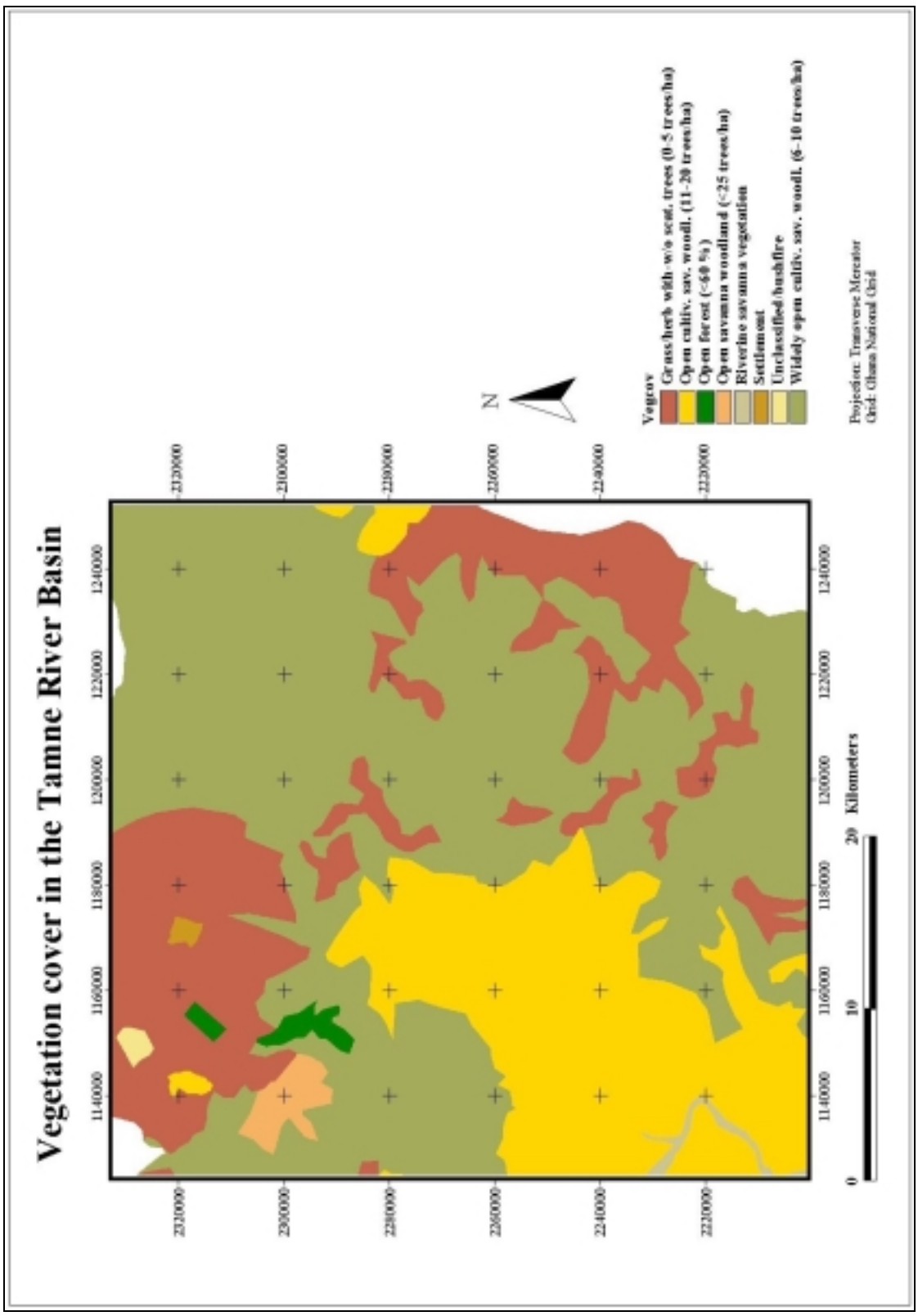
Vegcov
Grass/herb with w/o scat. trees (0-5 trees/ha)
Open cultiv. sav. woodl. (11-20 trees/ha)
Open forest (<60 %)
Open savanna woodland (<25 trees/ha)
Riverine savanna vegetation
Settlement
Unclassified/bushfire
Widely open cultiv. sav. woodl. (6-10 trees/ha)
N
Projection: Transverse Mercator
Grid: Ghana National Grid
Vegetation cover in the Tamne River Basin
2320000
2300000
2280000
2260000
2240000
2220000
1140000
1160000
1180000
1200000
1220000
1240000
0
10
20 Kilometers

Appendix 3

Main algorithm of the SteadyIndex application

```
Private tempN(810, 780) As Double
Private tempS(810, 780) As Double
Private tempE(810, 780) As Double
Private tempW(810, 780) As Double
Private tempNE(810, 780) As Double
Private tempSE(810, 780) As Double
Private tempNW(810, 780) As Double
Private tempSW(810, 780) As Double
Private visited(810, 780) As Boolean
Private result(810, 780) As Double
```

```
Public Sub CreateFile(row As Integer, col As Integer)
   Dim r As Integer
   Open "c:\temp\data\result.img" For Output As #1
   For r = 1 To row
      For c = 1 To col
      Write #1, result(r, c)
      Next c
   Next r
   Close #1
End Sub
```

```
Public Sub Calculate(N() As Double, E() As Double, S() As Double, W() As Double, NW() As
Double, NE() As Double, SW() As Double, SE() As Double, row As Integer, col As Integer, resol As
Integer)
   Dim count As Double
   count = 0
   Dim r As Integer
   Dim c As Integer
   Call Zero(row, col)
   For r = 1 To row
      For c = 1 To col
      visited(r, c) = True
      Call Trace(r, c, N, E, S, W, NW, NE, SW, SE, resol)
      result(r, c) = resol * resol + tempN(r + 1, c) + tempS(r - 1, c) + tempE(r, c - 1) + tempW(r, c + 1)
      +  tempNW(r + 1, c + 1) + tempNE(r + 1, c - 1) + tempSW(r - 1, c + 1) + tempSE(r - 1, c - 1)
      visited(r, c) = False
      count = count + 1
      Form1.Text5.Text = count
      Form1.Refresh
      Next c
   Next r
   Call createFile(row, col)
End Sub
```

```
Public Sub Zero(row As Integer, col As Integer)
   Dim r As Integer, c As Integer
   For r = 0 To row + 1
      For c = 0 To col + 1
      tempN(r, c) = 0
      tempS(r, c) = 0
      tempW(r, c) = 0
      tempE(r, c) = 0
      tempNE(r, c) = 0
      tempNW(r, c) = 0
      tempSE(r, c) = 0
      tempSW(r, c) = 0
      visited(r, c) = False
      Next c
   Next r
End Sub
```

```
Public Sub Trace(r As Integer, c As Integer, N() As Double, E() As Double, S() As Double, W() As
Double, NW() As Double, NE() As Double, SW() As Double, SE() As Double, resol As Integer)
   If (S(r - 1, c) <> 0) And (N(r, c) = 0) And (visited(r - 1, c) = False) And (tempS(r - 1, c) = 0) Then
      visited(r - 1, c) = True
      Call Trace(r - 1, c, N, E, S, W, NW, NE, SW, SE, resol)
      tempS(r - 1, c) = (resol * resol + tempS(r - 2, c) + tempW(r - 1, c + 1) + tempE(r - 1, c - 1) +
      tempNW(r,
      c + 1) + tempNE(r, c - 1) + tempSW(r - 2, c + 1) + tempSE(r - 2, c - 1)) * S(r - 1, c)
      visited(r - 1, c) = False
   End If
   If (W(r, c + 1) <> 0) And (E(r, c) = 0) And (visited(r, c + 1) = False) And (tempW(r, c + 1) = 0)
      Then
      visited(r, c + 1) = True
      Call Trace(r, c + 1, N, E, S, W, NW, NE, SW, SE, resol)
      tempW(r, c + 1) = (resol * resol + tempS(r - 1, c + 1) + tempN(r + 1, c + 1) + tempW(r, c + 2) +
      tempNW(r + 1, c + 2) + tempNE(r + 1, c) + tempSW(r - 1, c + 2) + tempSE(r - 1, c)) * W(r, c + 1)
      visited(r, c + 1) = False
   End If
   If (N(r + 1, c) <> 0) And (S(r, c) = 0) And (visited(r + 1, c) = False) And (tempN(r + 1, c) = 0) Then
      visited(r + 1, c) = True
      Call Trace(r + 1, c, N, E, S, W, NW, NE, SW, SE, resol)
      tempN(r + 1, c) = (resol * resol + tempN(r + 2, c) + tempW(r + 1, c + 1) + tempE(r + 1, c - 1) +
      tempNW(r + 2, c + 1) + tempNE(r + 2, c - 1) + tempSW(r, c + 1) + tempSE(r, c - 1)) * N(r + 1, c)
      visited(r + 1, c) = False
   End If
   If (E(r, c - 1) <> 0) And (W(r, c) = 0) And (visited(r, c - 1) = False) And (tempE(r, c - 1) = 0) Then
      visited(r, c - 1) = True
      Call Trace(r, c - 1, N, E, S, W, NW, NE, SW, SE, resol)
      tempE(r, c - 1) = (resol * resol + tempS(r - 1, c - 1) + tempN(r + 1, c - 1) + tempE(r, c - 2) +
      tempNW(r
      + 1, c) + tempNE(r + 1, c - 2) + tempSW(r - 1, c) + tempSE(r - 1, c - 2)) * E(r, c - 1)
      visited(r, c - 1) = False
   End If
   If (NE(r + 1, c - 1) <> 0) And (SW(r, c) = 0) And (visited(r + 1, c - 1) = False) And (tempNE(r + 1,
      c- 1) = 0) Then
      visited(r + 1, c - 1) = True
      Call Trace(r + 1, c - 1, N, E, S, W, NW, NE, SW, SE, resol)
      tempNE(r + 1, c - 1) = (resol * resol + tempS(r, c - 1) + tempN(r + 2, c - 1) + tempW(r + 1, c) +
      tempE(r + 1, c - 2) + tempNW(r + 2, c) + tempNE(r + 2, c - 2) + tempSE(r, c - 2)) * NE(r + 1, c
      +1)
      visited(r + 1, c - 1) = False
   End If
```

```
    If (NW(r + 1, c + 1) <> 0) And (SE(r, c) = 0) And (visited(r + 1, c + 1) = False) And (tempNW(r + 1,
       c + 1) = 0) Then
       visited(r + 1, c + 1) = True
       Call Trace(r + 1, c + 1, N, E, S, W, NW, NE, SW, SE, resol)
       tempNW(r + 1, c + 1) = (resol * resol + tempS(r, c + 1) + tempN(r + 2, c + 1) + tempW(r + 1, c +
       2) + tempE(r + 1, c) + tempNW(r + 2, c + 2) + tempSW(r, c + 2) + tempNE(r + 2, c)) * NW(r + 1,
       c + 1)
       visited(r + 1, c + 1) = False
    End If
    If (SE(r - 1, c - 1) <> 0) And (NW(r, c) = 0) And (visited(r - 1, c - 1) = False) And (tempSE(r - 1, c –
       1) = 0) Then
       visited(r - 1, c - 1) = True
       Call Trace(r - 1, c - 1, N, E, S, W, NW, NE, SW, SE, resol)
       tempSE(r - 1, c - 1) = (resol * resol + tempS(r - 2, c - 1) + tempN(r, c - 1) + tempW(r - 1, c) +
       tempE(r – 1, c - 2) + tempNE(r, c - 2) + tempSW(r - 2, c) + tempSE(r - 2, c - 2)) * SE(r - 1, c - 1)
       visited(r - 1, c - 1) = False
    End If
    If (SW(r - 1, c + 1) <> 0) And (NE(r, c) = 0) And (visited(r - 1, c + 1) = False) And (tempSW(r - 1, c
       + 1) = 0) Then
       visited(r - 1, c + 1) = True
       Call Trace(r - 1, c + 1, N, E, S, W, NW, NE, SW, SE, resol)
       tempSW(r - 1, c + 1) = (resol * resol + tempS(r - 2, c + 1) + tempN(r, c + 1) + tempW(r - 1, c + 2)
       + tempE(r - 1, c) + tempNW(r, c + 2) + tempSW(r - 2, c + 2) + tempSE(r - 2, c)) * SW(r - 1, c + 1)
       visited(r - 1, c + 1) = False
    End If
End Sub
```

Main algorithm of the NonSteadyIndex application

```
Private tempN(810, 780) As Double
Private tempS(810, 780) As Double
Private tempE(810, 780) As Double
Private tempW(810, 780) As Double
Private tempNE(810, 780) As Double
Private tempSE(810, 780) As Double
Private tempNW(810, 780) As Double
Private tempSW(810, 780) As Double
Private visited(810, 780) As Boolean
Private include(810, 780) As Boolean
Private result(100) As Double
```

```
Public Sub CreateFile(ends As Integer)
    Dim r As Integer
    Open "c:\temp\data\result.img" For Output As #1
    For r = 1 To ends
       Write #1, result(r)
    Next r
    Close #1
End Sub
```

```
Public Sub Calculate(N() As Double, E() As Double, S() As Double, W() As Double, NW() As
Double, NE() As Double, SW() As Double, SE() As Double, time() As Double, time2 As Integer, row
As Integer, col As Integer, resol As Integer, ro() As Integer, co() As Integer, ends As Integer)

    Dim count As Double
    Dim r As Integer
    Dim c As Integer
```

```
    count = 0
    cumT = 0
    Dim rr As Integer
    For rr = 1 To ends
        include(ro(rr), co(rr)) = True
        visited(ro(rr), co(rr)) = True
        Call GetArea(ro(rr), co(rr), N, E, S, W, NW, NE, SW, SE, time, time2)
        Call Trace(ro(rr), co(rr), N, E, S, W, NW, NE, SW, SE, resol)
        r = ro(rr)
        c = co(rr)
        result(rr) = resol * resol + tempN(r + 1, c) + tempS(r - 1, c) + tempE(r, c - 1) + tempW(r, c + 1) +
        tempNW(r + 1, c + 1) + tempNE(r + 1, c - 1) + tempSW(r - 1, c + 1) + tempSE(r - 1, c - 1)
        Call Zero(row, col)
        count = count + 1
        Form1.Text8.Text = count
        Form1.Refresh
    Next rr
    Call CreateFile(ends)
End Sub
```

```
Public Sub GetArea(r As Integer, c As Integer, N() As Double, E() As Double, S() As Double, W() As
Double, NW() As Double, NE() As Double, SW() As Double, SE() As Double, time() As Double,
time2 As Integer)
If (S(r - 1, c) <> 0) And (N(r, c) = 0) And (include(r - 1, c) = False) Then
        cumT = cumT + time(r - 1, c)
        If (cumT <= time2) Then
            Call GetArea(r - 1, c, N, E, S, W, NW, NE, SW, SE, time, time2)
            include(r - 1, c) = True
        End If
        cumT = cumT - time(r - 1, c)
End If
If (W(r, c + 1) <> 0) And (E(r, c) = 0) And (include(r, c + 1) = False) Then
        cumT = cumT + time(r, c + 1)
        If (cumT <= time2) Then
            Call GetArea(r, c + 1, N, E, S, W, NW, NE, SW, SE, time, time2)
            include(r, c + 1) = True
        End If
        cumT = cumT - time(r, c + 1)
End If
If (N(r + 1, c) <> 0) And (S(r, c) = 0) And (include(r + 1, c) = False) Then
        cumT = cumT + time(r + 1, c)
        If (cumT <= time2) Then
            Call GetArea(r + 1, c, N, E, S, W, NW, NE, SW, SE, time, time2)
            include(r + 1, c) = True
        End If
        cumT = cumT - time(r + 1, c)
End If
If (E(r, c - 1) <> 0) And (W(r, c) = 0) And (include(r, c - 1) = False) Then
        cumT = cumT + time(r, c - 1)
        If (cumT <= time2) Then
            Call GetArea(r, c - 1, N, E, S, W, NW, NE, SW, SE, time, time2)
            include(r, c - 1) = True
        End If
        cumT = cumT - time(r, c - 1)
End If
If (NE(r + 1, c - 1) <> 0) And (SW(r, c) = 0) And (include(r + 1, c - 1) = False) Then
        cumT = cumT + time(r + 1, c - 1)
        If (cumT <= time2) Then
            Call GetArea(r + 1, c - 1, N, E, S, W, NW, NE, SW, SE, time, time2)
```

```
        include(r + 1, c - 1) = True
      End If
      cumT = cumT - time(r + 1, c - 1)
End If
If (NW(r + 1, c + 1) <> 0) And (SE(r, c) = 0) And (include(r + 1, c + 1) = False) Then
      cumT = cumT + time(r + 1, c + 1)
      If (cumT <= time2) Then
        Call GetArea(r + 1, c + 1, N, E, S, W, NW, NE, SW, SE, time, time2)
        include(r + 1, c + 1) = True
      End If
      cumT = cumT - time(r + 1, c + 1)
End If
If (SE(r - 1, c - 1) <> 0) And (NW(r, c) = 0) And (include(r - 1, c - 1) = False) Then
      cumT = cumT + time(r - 1, c - 1)
      If (cumT <= time2) Then
        Call GetArea(r - 1, c - 1, N, E, S, W, NW, NE, SW, SE, time, time2)
        include(r - 1, c - 1) = True
      End If
      cumT = cumT - time(r - 1, c - 1)
End If
If (SW(r - 1, c + 1) <> 0) And (NE(r, c) = 0) And (include(r - 1, c + 1) = False) Then
      cumT = cumT + time(r - 1, c + 1)
      If (cumT <= time2) Then
        Call GetArea(r - 1, c + 1, N, E, S, W, NW, NE, SW, SE, time, time2)
        include(r - 1, c + 1) = True
      End If
      cumT = cumT - time(r - 1, c + 1)
End If
End Sub
```

```
Public Sub Zero(row As Integer, col As Integer)
   Dim r As Integer, c As Integer
   For r = 0 To row + 1
      For c = 0 To col + 1
      tempN(r, c) = 0
      tempS(r, c) = 0
      tempW(r, c) = 0
      tempE(r, c) = 0
      tempNE(r, c) = 0
      tempNW(r, c) = 0
      tempSE(r, c) = 0
      tempSW(r, c) = 0
      visited(r, c) = False
      include(r, c) = False
      Next c
   Next r
End Sub
```

```
Public Sub Trace(r As Integer, c As Integer, N() As Double, E() As Double, S() As Double, W() As
Double, NW() As Double, NE() As Double, SW() As Double, SE() As Double, resol As Integer)
   If (S(r - 1, c) <> 0) And (N(r, c) = 0) And (visited(r - 1, c) = False) And (tempS(r - 1, c) = 0) And
   (include(r - 1, c) = True) Then
      visited(r - 1, c) = True
      Call Trace(r - 1, c, N, E, S, W, NW, NE, SW, SE, resol)
      tempS(r - 1, c) = (resol * resol + tempS(r - 2, c) + tempW(r - 1, c + 1) + tempE(r - 1, c - 1) +
      tempNW(r, c + 1) + tempNE(r, c - 1) + tempSW(r - 2, c + 1) + tempSE(r - 2, c - 1)) * S(r - 1, c)
      visited(r - 1, c) = False
   End If
```

```
    If (W(r, c + 1) <> 0) And (E(r, c) = 0) And (visited(r, c + 1) = False) And (tempW(r, c + 1) = 0) And
    (include(r, c + 1) = True) Then
        visited(r, c + 1) = True
        Call Trace(r, c + 1, N, E, S, W, NW, NE, SW, SE, resol)
        tempW(r, c + 1) = (resol * resol + tempS(r - 1, c + 1) + tempN(r + 1, c + 1) + tempW(r, c + 2) +
        tempNW(r + 1, c + 2) + tempNE(r + 1, c) + tempSW(r - 1, c + 2) + tempSE(r - 1, c)) * W(r, c + 1)
        visited(r, c + 1) = False
    End If
    If (N(r + 1, c) <> 0) And (S(r, c) = 0) And (visited(r + 1, c) = False) And (tempN(r + 1, c) = 0) And
    (include(r + 1, c) = True) Then
        visited(r + 1, c) = True
        Call Trace(r + 1, c, N, E, S, W, NW, NE, SW, SE, resol)
        tempN(r + 1, c) = (resol * resol + tempN(r + 2, c) + tempW(r + 1, c + 1) + tempE(r + 1, c - 1) +
        tempNW(r + 2, c + 1) + tempNE(r + 2, c - 1) + tempSW(r, c + 1) + tempSE(r, c - 1)) * N(r + 1, c)
        visited(r + 1, c) = False
    End If
    If (E(r, c - 1) <> 0) And (W(r, c) = 0) And (visited(r, c - 1) = False) And (tempE(r, c - 1) = 0) And
    (include(r, c - 1) = True) Then
        visited(r, c - 1) = True
        Call Trace(r, c - 1, N, E, S, W, NW, NE, SW, SE, resol)
        tempE(r, c - 1) = (resol * resol + tempS(r - 1, c - 1) + tempN(r + 1, c - 1) + tempE(r, c - 2) +
        tempNW(r + 1, c) + tempNE(r + 1, c - 2) + tempSW(r - 1, c) + tempSE(r - 1, c - 2)) * E(r, c - 1)
        visited(r, c - 1) = False
    End If
    If (NE(r + 1, c - 1) <> 0) And (SW(r, c) = 0) And (visited(r + 1, c - 1) = False) And (tempNE(r + 1, c
        - 1)  = 0) And (include(r + 1, c - 1) = True) Then
        visited(r + 1, c - 1) = True
        Call Trace(r + 1, c - 1, N, E, S, W, NW, NE, SW, SE, resol)
        tempNE(r + 1, c - 1) = (resol * resol + tempS(r, c - 1) + tempN(r + 2, c - 1) + tempW(r + 1, c) +
        tempE(r + 1, c - 2) + tempNW(r + 2, c) + tempNE(r + 2, c - 2) + tempSE(r, c - 2)) * NE(r + 1, c –
        1)
        visited(r + 1, c - 1) = False
    End If
    If (NW(r + 1, c + 1) <> 0) And (SE(r, c) = 0) And (visited(r + 1, c + 1) = False) And (tempNW(r + 1,
        c + 1) = 0) And (include(r + 1, c + 1) = True) Then
        visited(r + 1, c + 1) = True
        Call Trace(r + 1, c + 1, N, E, S, W, NW, NE, SW, SE, resol)
        tempNW(r + 1, c + 1) = (resol * resol + tempS(r, c + 1) + tempN(r + 2, c + 1) + tempW(r + 1, c +
        2) + tempE(r + 1, c) + tempNW(r + 2, c + 2) + tempSW(r, c + 2) + tempNE(r + 2, c)) * NW(r + 1,
        c + 1)
        visited(r + 1, c + 1) = False
    End If
    If (SE(r - 1, c - 1) <> 0) And (NW(r, c) = 0) And (visited(r - 1, c - 1) = False) And (tempSE(r - 1, c –
        1) = 0) And (include(r - 1, c - 1) = True) Then
        visited(r - 1, c - 1) = True
        Call Trace(r - 1, c - 1, N, E, S, W, NW, NE, SW, SE, resol)
        tempSE(r - 1, c - 1) = (resol * resol + tempS(r - 2, c - 1) + tempN(r, c - 1) + tempW(r - 1, c) +
        tempE(r  - 1, c - 2) + tempNE(r, c - 2) + tempSW(r - 2, c) + tempSE(r - 2, c - 2)) * SE(r - 1, c - 1)
        visited(r - 1, c - 1) = False
    End If
    If (SW(r - 1, c + 1) <> 0) And (NE(r, c) = 0) And (visited(r - 1, c + 1) = False) And (tempSW(r - 1, c
        + 1) = 0) And (include(r - 1, c + 1) = True) Then
        visited(r - 1, c + 1) = True
        Call Trace(r - 1, c + 1, N, E, S, W, NW, NE, SW, SE, resol)
        tempSW(r - 1, c + 1) = (resol * resol + tempS(r - 2, c + 1) + tempN(r, c + 1) + tempW(r - 1, c + 2)
        + tempE(r - 1, c) + tempNW(r, c + 2) + tempSW(r - 2, c + 2) + tempSE(r - 2, c)) * SW(r - 1, c + 1)
        visited(r - 1, c + 1) = False
    End If
End Sub
```

Appendix 4

Transect A

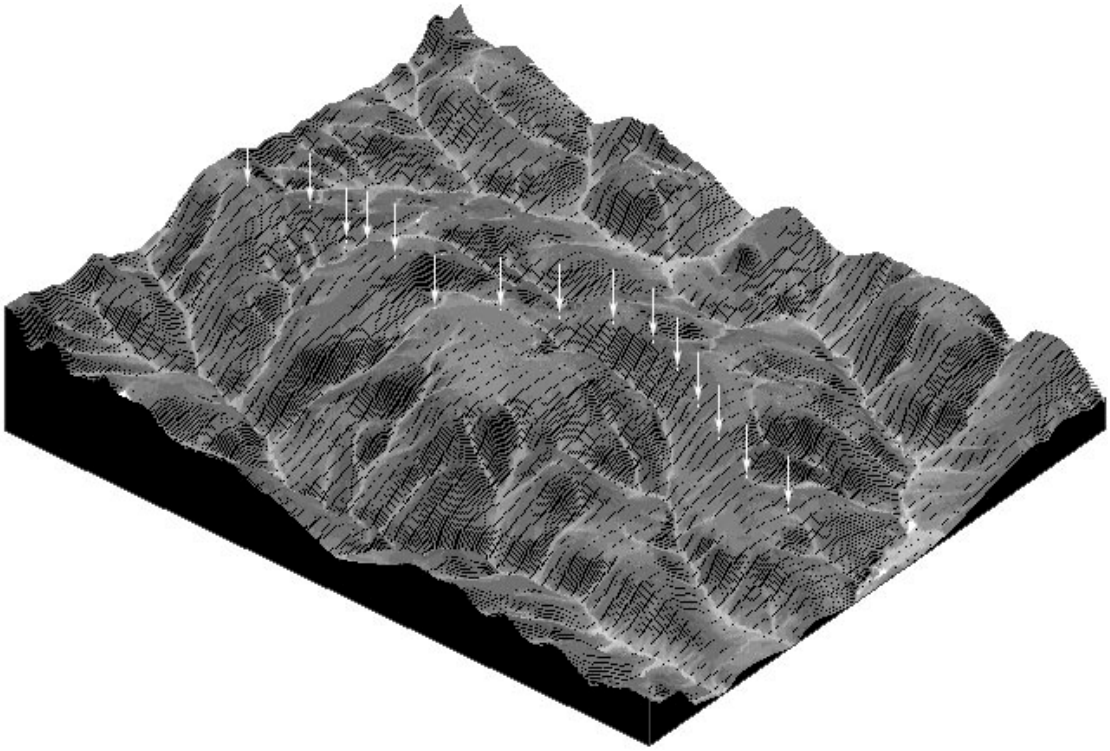

Transect B

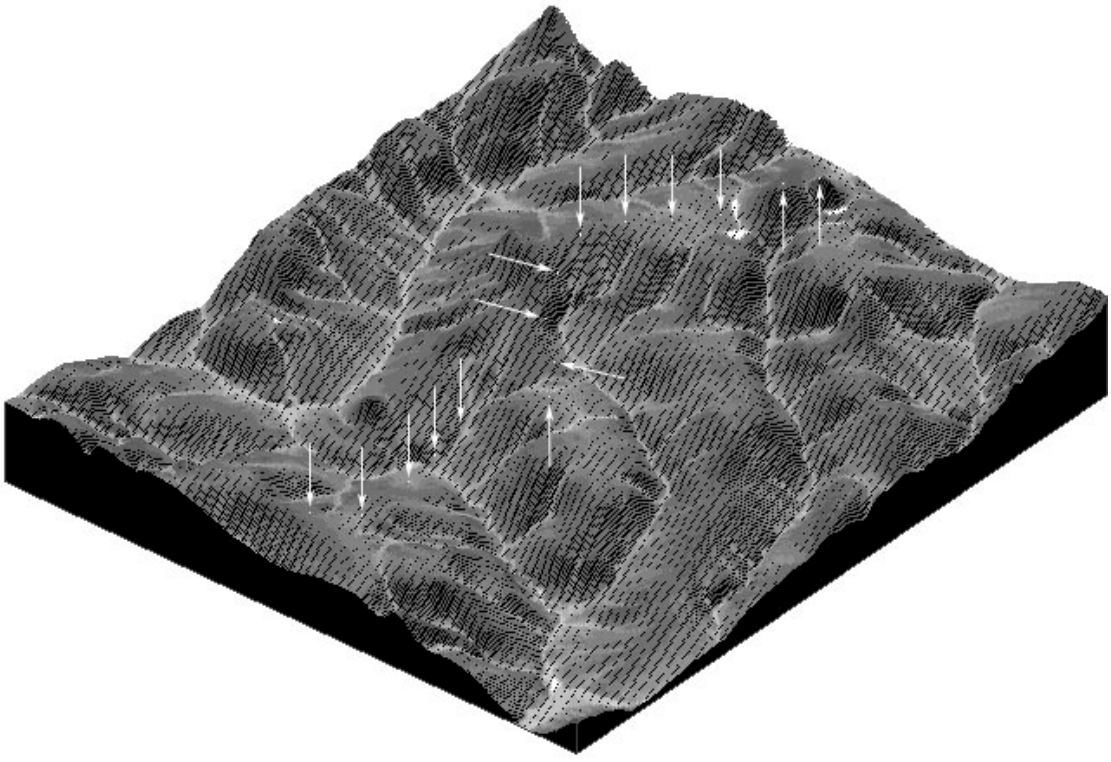

Transect C

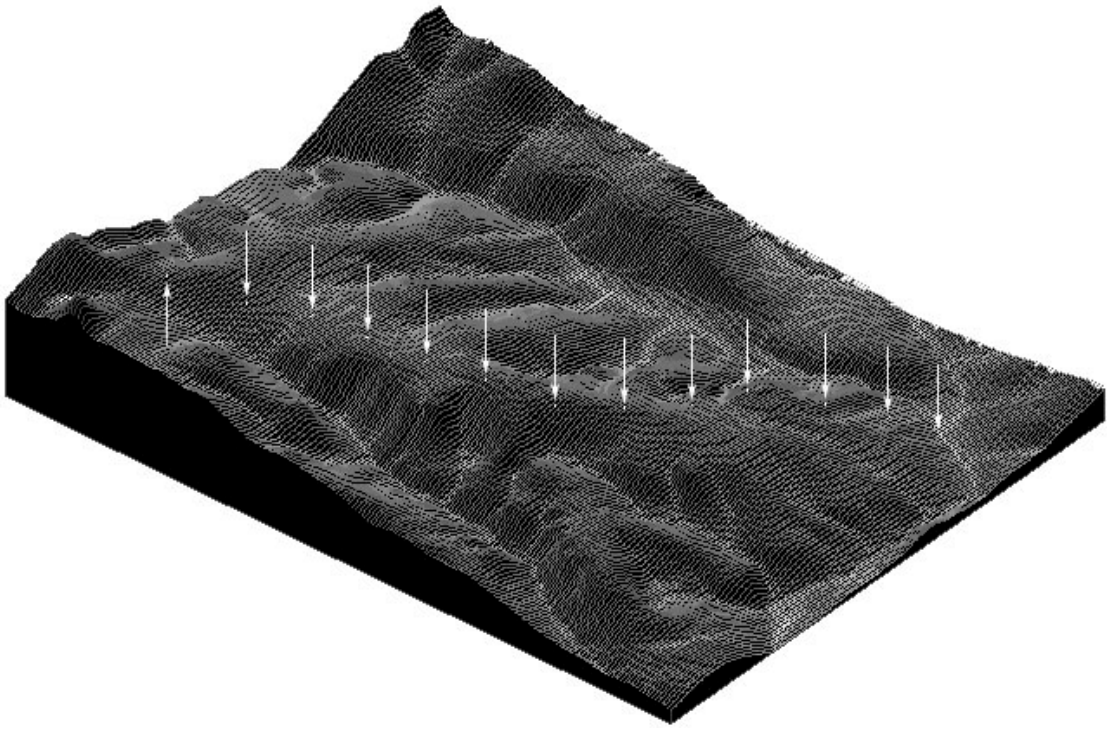

Transect E

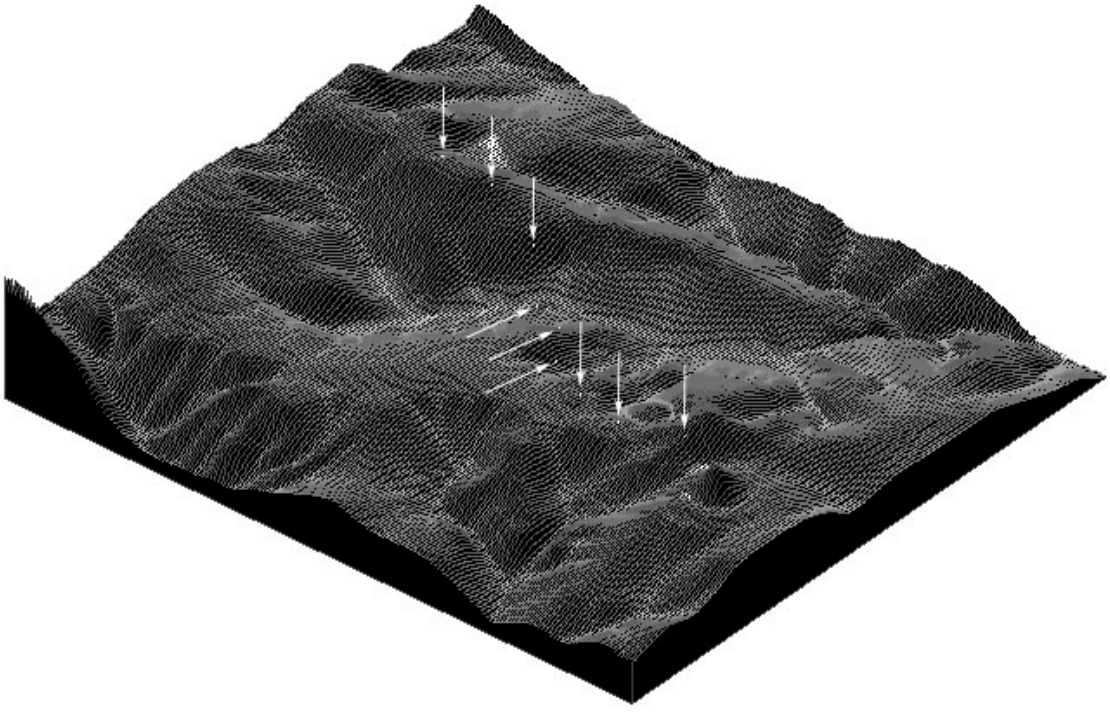

Transect F

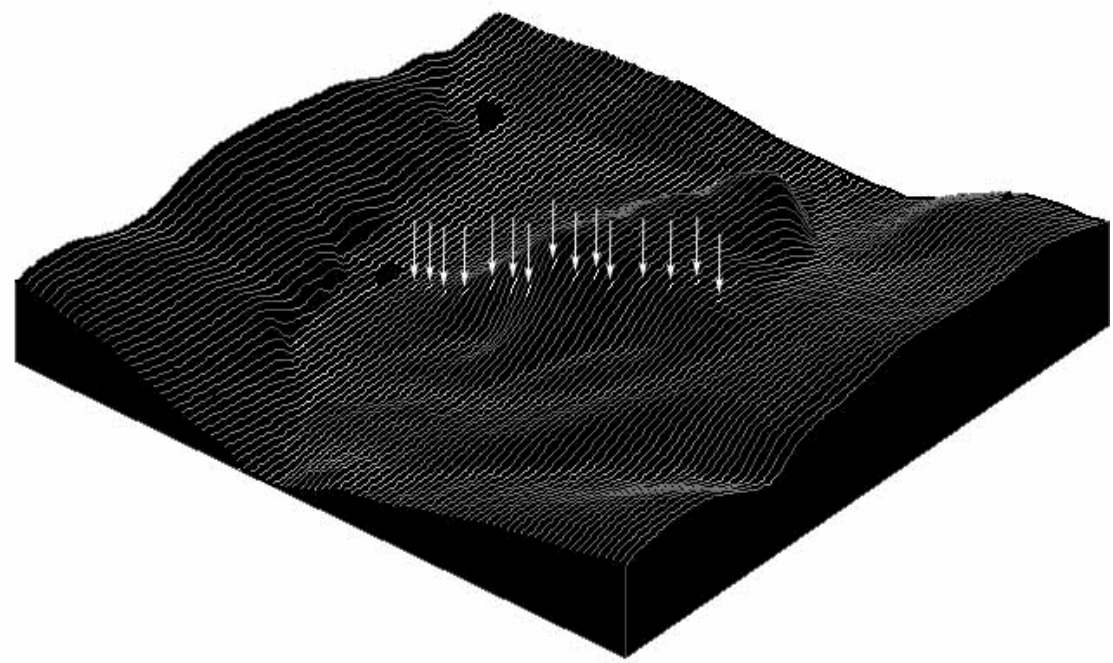

Transect G

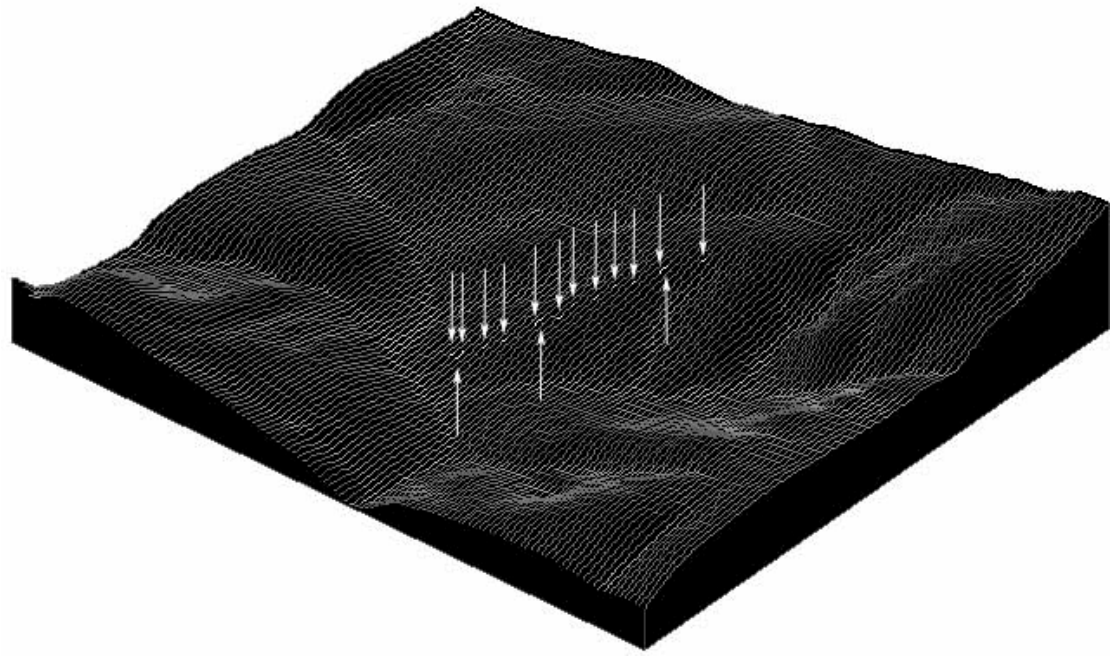

Transect H